The effect of anthropogenic emission, meteorological factors, and carbon dioxide on the surface ozone increase in China from 2008 to 2018 during the East Asia summer monsoon season

Danyang Ma[1], Tijian Wang[1,*], Hao Wu[2], Yawei Qu[3], Jian Liu[4], Jane Liu[5], Shu Li[1], Bingliang Zhuang[1], Mengmeng Li[1], Min Xie[1]

[1]School of Atmospheric Sciences, Nanjing University, Nanjing 210023, China.

[2]Key Laboratory of Transportation Meteorology of China Meteorological Administration, Nanjing Joint Institute for Atmospheric Sciences, Nanjing 210000, China.

[3]College of Intelligent Science and Control Engineering, Jinling Institute of Technology, Nanjing 211169, China.

[4]Key Laboratory for Virtual Geographic Environment of Ministry of Education;Jiangsu Center for Collaborative Innovation in Geographical Information Resource Development and Application;School of Geography Science, Nanjing Normal University, Nanjing, China 210023.

[5]Department of Geography and Planning, University of Toronto, Toronto M5S 2E8, Canada.

Correspondence to: Tijian Wang (tjwang@nju.edu.cn)

Abstract. Despite the implementation of the Clean Air Action Plan by the Chinese government in 2013, the issue of increasing surface ozone (O_3) concentrations remains a significant environmental concern in China. In this study, we used an improved regional climate-chemistry-ecology model (RegCM-Chem-YIBs) to investigate the impact of anthropogenic emissions, meteorological factors, and CO_2 changes on summer surface O_3 levels in China from 2008 to 2018. Compared to its predecessor, the model has been enhanced concerning the photolysis of O_3 and the radiative impacts of CO_2 and O_3. The investigations showed anthropogenic emissions were the primary contributor to the O_3 increase in China, responsible for 4.08~18.51 ppb in the North China Plain. However, changed meteorological conditions played a crucial role in decreasing O_3 in China and may have a more significant impact than anthropogenic emissions in some regions. Changed CO_2 played a critical role in the variability of O_3 through radiative forcing and isoprene emissions, particularly in southern China, inducing an increase in O_3 on the southeast coast of China (0.28~0.46 ppb) and a decrease in the southwest and central China (-0.51~-0.11 ppb). Our study comprehensively analyzed O_3 variation across China from various perspectives and highlighted the importance of considering CO_2 variations when designing long-term O_3 control policies, especially in high vegetation coverage areas.

1 Introduction

O_3 is a strong oxidant detrimental to human health (Lu et al., 2020; Liu et al., 2018a) and vegetation growth (Monks et al., 2015; Wang et al., 2017a). Furthermore, it is a crucial active compound influencing the earth's radiative balance, with an effective radiative forcing of up to 0.47 W/m^2 in 2019 (Ipcc, 2021). Tropospheric O_3 has garnered significant attention over the past few decades due to its crucial role in air quality and climate change (Duan et al., 2017; Li et al., 2019; Ashmore and Bell, 1991; Lu et al., 2018).

With the rapid development in China, emissions of O_3 precursors have been on the rise, leading to an annual increase in O_3 concentrations since the beginning of the 20th century (Liu and Wang, 2020a; Ma et al., 2016). Surface O_3 pollution has become a severe air quality concern in China (Verstraeten et al., 2016; Xu et al., 2018), particularly in major urban areas such as the North China Plain (NCP), Fenwei Plain (FWP), Yangtze River Delta (YRD), Pearl River Delta (PRD), and the Sichuan Basin (SCB) (Wang et al., 2020; Wang et al., 2017a; Yin and Ma, 2020; Shen et al., 2019; Zhao et al., 2018; Wang et al., 2009). Although the Chinese government initialized the Clean Air Action Plan in 2013 to control air pollution, the concentration of O_3 precursors and $PM_{2.5}$ has significantly decreased (Zhai et al., 2019). However, surface O_3 concentrations continue to increase in major urban areas.

Recent studies have suggested that regional meteorological conditions influence surface O_3 levels through various pathways (Jacob and Winner, 2009; Shen et al., 2016; Lin et al., 2008). Modeling studies have shown that O_3 levels are sensitive to temperature, humidity, wind speed, mixing height, and other meteorological conditions (Pfister et al., 2014; Sanchez-Ccoyllo et al., 2006). For instance, temperature affects the chemical formation rate of O_3 (Lee et al., 2014), while precipitation reduces surface O_3 concentrations through wet removal (Fang et al., 2011). Additionally, the elevated planetary boundary layer (PBL) height enhances upward movement, resulting in lower surface O_3 concentrations (Haman et al., 2014). Therefore, long-term modeling of surface O_3 levels must consider changes in meteorological conditions.

57   CO_2 is the primary anthropogenic radiative force of the climate system (Gauss et al., 2003;
58 Schimel et al., 2015). CO_2 can impact regional air temperature and precipitation, leading to
59 changes in surface O_3 concentrations (Lu et al., 2013; Yang et al., 2014).

60   On the other hand, Biogenic volatile organic compounds (BVOCs) are significant O_3
61 precursors, and isoprene is the primary specie among BVOCs that vegetation emits (Zheng et al.,
62 2009; Fiore et al., 2011). In most of China, O_3 is volatile organic compounds (VOCs)-limited in
63 the summer, especially in industrial cities (Li et al., 2018; Wu et al., 2018). Thus, it plays a
64 significant role in modulating O_3 levels and positively correlates with O_3 concentrations in major
65 urban areas of China. It is known that CO_2 can enhance vegetation's photosynthesis (Sun et al.,
66 2013; Heald et al., 2009; Tai et al., 2013; Monson and Fall, 1989), which may directly increase
67 isoprene emission (Rapparini et al., 2004). Based on the observation, Rosenstiel et al. (2003)
68 found that the isoprene emissions of plants grew by about 21% and 41% when CO_2 reached 800
69 ppm and 1200 ppm, respectively. However, Wilkinson et al. (2009) indicated that different
70 vegetation types show varying responses in isoprene emission when CO_2 increases. Isoprene
71 emission was decreased by 30~40% in Populus tremuloides Michx but increased by about 100%
72 in Quercus rubra when CO_2 concentrations were grown (Sharkey et al., 1991). High
73 concentrations of CO_2 may inhibit the emission of isoprene by reducing the activity of BVOCs
74 synthetase or decreasing the synthesis of adenosine triphosphate (Possell et al., 2005). Guenther
75 et al. (1991) also indicated that isoprene emissions were significantly reduced when CO_2 was
76 increased from 100 to 600 µmol mol^{-1}. In summary, the impact of elevated CO_2 on isoprene
77 emission may be positive or negative, mainly related to the relative size of the inhibition caused
78 by elevated CO_2 and promotion by enhanced photosynthesis.

79   Numerous studies have concluded that anthropogenic emissions are the primary drivers of
80 surface O_3 increases in different regions or years in China. Meanwhile, the effects of
81 meteorological parameters can be substantial (Wang et al., 2019c; Lu et al., 2019; Dang et al.,
82 2021; Liu and Wang, 2020a). For instance, Li et al. (2020) indicated that anthropogenic
83 emissions were the primary cause of surface O_3 increase in China from 2013 to 2019. Liu and
84 Wang (2020a) suggested that anthropogenic emissions play a dominant role in the O_3 variety in
85 China, but the effects of meteorological conditions could be more significant in some regions.
86 Han et al. (2020) analyzed the O_3 changes in summer and suggested that meteorology can
87 explain about 43% of that in eastern China.

88   Previous studies have mainly focused on the impact of anthropogenic emissions and
89 meteorological factors on the rise of O_3 levels, with limited attention given to the role of CO_2
90 variations. However, due to the rapid socioeconomic growth in China and the subsequent surge
91 in energy consumption, CO_2 emissions, and concentrations have also increased significantly,
92 particularly in the eastern coastal region (Lv et al., 2020; Ren et al., 2014). Furthermore, given
93 the significant impact of CO_2 on O_3, it is crucial to evaluate the influence of changes in CO_2
94 concentration on the maximum daily 8-hour average (MDA8) O_3 concentrations at the surface.
95 Thus, a comprehensive assessment of the impact of anthropogenic emissions, meteorological
96 factors, and CO_2 on surface O_3 is imperative.

97   Here, we employed an advanced regional climate-chemistry-ecology model to assess the
98 impact of anthropogenic emissions, meteorological factors, and carbon dioxide variations during
99 the summer monsoon period (May, June, July, and August) on surface O_3 levels. Our findings
100 can facilitate the development of a comprehensive O_3 improvement strategy. Sect. 2 describes

101 the methods and data, and the results and discussion are given in Sect. 3, finally, the conclusions
102 are shown in Sect. 4.

2 Methods and data

104 2.1 Measurement data

105 We compared the simulated regional meteorological factors with the European Centre for
106 Medium-Range Weather Forecasts Interim reanalysis data (ERA-Interim) at 37 vertical levels,
107 which included temperature, relative humidity, and wind speed (Balsamo et al., 2015; Hoffmann
108 et al., 2019). The observed surface O_3 was taken from the China National Environmental
109 Monitoring Center (CNEMC), which had more than 1400 environmental monitoring stations in
110 2018 (Wang et al., 2018; Kong et al., 2021; Zheng et al., 2014). The World Data Centre for
111 Greenhouse Gases (WDCGG) data (Liu et al., 2009; Li et al., 2017) was applied to evaluate the
112 simulated surface CO_2 concentrations. The monitoring stations of O_3 and CO_2 are shown in
113 Figure. 1.

114
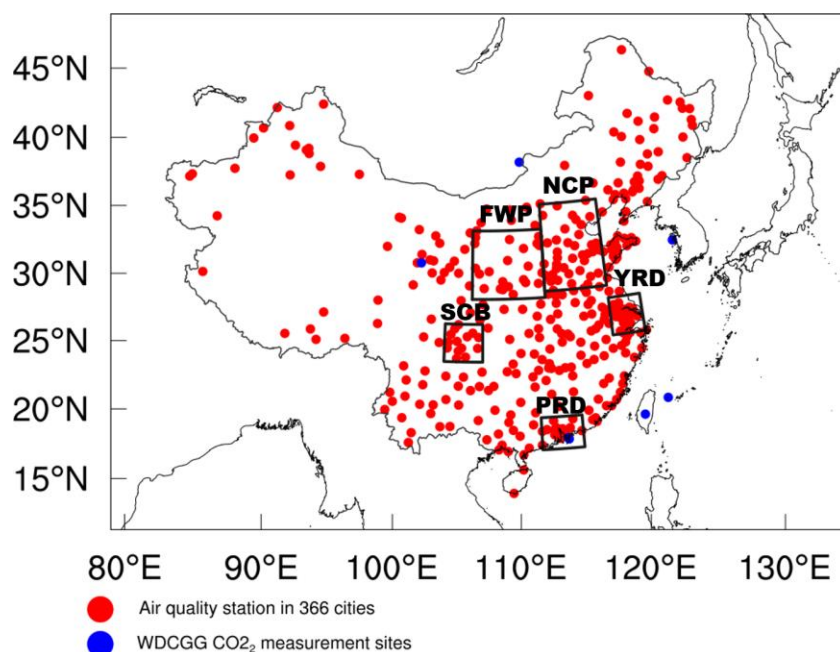
115
116 **Figure 1.** Model domains for the RegCM-Chem-YIBs model. The regions with black boundaries are the
117 North China Plain (34~41°N, 113~119°E), the Yangtze River Delta (30~33°N, 119~122°E), the Pearl
118 River Delta (21.5~24°N, 112~115.5°E), the Sichuan Basin (28.5~31.5°N, 103.5~107°E), and the Fenwei
119 Plain (33.5~39°N, 106~113°E) regions.

120 2.2 Model description

121 The RegCM-Chem-YIBs is a regional climate-chemistry-ecology model developed from the
122 RegCM model. RegCM is a regional climate model initially developed by the International
123 Center for Theoretical Physics (ICTP) (Giorgi et al., 2012). Shalaby et al. (2012) integrated the
124 Chem chemistry model into the RegCM model and incorporated the condensed version of the
125 Carbon Bond Mechanism (CBM-Z) to enhance the model's capabilities. To further improve the
126 model's performance, Yin et al. (2015) added a Volatility Basis Set (VBS) scheme to simulate
127 Secondary Organic Aerosols (SOA). Xie et al. (2020) further modified the model by

128 incorporating CO_2 as a tracer, which is subject to regulation by sources, sinks, and atmospheric
129 transport processes. The model represents the four sources and sinks of CO_2 as surface fluxes,
130 including emissions from fossil fuels and biomass burning, air-sea CO_2 exchange, and terrestrial
131 biosphere CO_2 fluxes. Additionally, the model incorporated the Yale Interactive Terrestrial
132 Biosphere (YIBs), a land carbon cycle model that enables the simulation of ecological processes,
133 including carbon assimilation, allocation, and autotrophic and heterotrophic respiration (Yue and
134 Unger, 2015).

135 The ecological model (YIBs) was fully coupled into the regional climate-chemical model
136 (RegCM-Chem) to reproduce the interactions between atmospheric composition and the
137 ecosystem in the actual atmosphere (Xie et al., 2019). The meteorological factors and air
138 components simulated by RegCM-Chem were input into the YIBs model to simulate vegetation
139 physiological processes and calculate land surface parameters such as carbon dioxide flux,
140 BVOCs emissions, and stomatal conductance. Conversely, the simulations of the YIBs model
141 were fed back into the RegCM-Chem model to adjust the air qualities, temperature, humidity,
142 circulation, and other meteorological fields. The RegCM-Chem-YIBs has been extensively
143 applied to study surface O_3, $PM_{2.5}$, CO_2, the summer monsoon, and the interactions between air
144 quality and the ecosystem (Zhuang et al., 2018; Pu et al., 2017; Xu et al., 2022a; Xie et al., 2018;
145 Ma et al., 2023).

146 The RegCM model offers a variety of physical and chemical parameterization options. Here,
147 the climatological chemical boundary conditions were driven by the Model of Ozone and
148 Related Chemical Tracers (MOZART). The gas-phase chemistry employed the CBM-Z scheme
149 (Zaveri and Peters, 1999). For the boundary layer scheme, the Holtslag PBL approach was
150 utilized (Khayatianyazdi et al., 2021). The Grell cumulus convection scheme was employed to
151 simulate convective processes (Grell, 1993). The CCM3 radiation scheme and CLM3.5 land
152 surface module were used in the model (Collins et al., 2006; Giorgi and Mearns, 1999; Decker
153 and Zeng, 2009).

154 2.3 Model improvements

155 2.3.1 Radiation

156 In the previous version of the RegCM-Chem-YIBs model, radiative calculations only
157 accounted for changes in the spatiotemporal distribution of particulate matter. To simplify the
158 radiation calculations, the atmospheric CO_2 and O_3 concentrations were assumed to be constant
159 throughout the year. However, atmospheric CO_2 and O_3 are subject to modulation by various
160 sources, sinks, physical processes, and chemical processes (Ballantyne et al., 2012; Wang et al.,
161 2019a). Additionally, rapid urbanization in China has led to an annual increase in CO_2 and O_3
162 concentrations (Guan et al., 2021; Wei et al., 2022), with elevated concentrations and growth
163 rates primarily distributed in the eastern regions where urbanization is most prominent (Shi et al.,
164 2016; Wang et al., 2017b). To more accurately simulate the atmospheric radiation balance and
165 East Asian monsoon climate, it is necessary to incorporate spatiotemporal variations of CO_2 and
166 O_3 concentrations into the radiation module. Therefore, we included the varying CO_2 and O_3
167 concentrations simulated by the model in the radiation module to calculate the corresponding
168 radiative forcing.

169 2.3.2 Photolysis

170 The photolysis process was simulated using the Tropospheric Ultraviolet and Visible (TUV)

171   model, which is commonly used to compute photolysis rates in various models (Tie et al., 2003;
172   Shetter et al., 2002; Borg et al., 2011). The TUV model employs input parameters such as zenith
173   angle, altitude, ozone column, SO_2 column, NO_2 column, aerosol optical depth (AOD), single
174   scattering albedo (SSA), and albedo, among others, to calculate photolysis rates (Singh and
175   Singh, 2004). However, in the TUV module of the RegCM-Chem-YIBs model, AOD and SSA
176   were held constant. This is problematic as accurate aerosol optical parameters, such as AOD and
177   SSA, play a crucial role in the photolysis of O_3 (Lefer et al., 2003). To address this issue, we
178   incorporated temporally and spatially varying AOD and SSA simulated by the RegCM-Chem-
179   YIBs model into the photolysis rate calculations in the TUV module. This enabled us to
180   accurately incorporate the extinction effect of the varying particles into the photolysis reaction,
181   leading to more realistic simulations of air components and regional meteorology.

182   2.4 Emissions and Experiment settings

183   Anthropogenic emissions from 2008 to 2018 were obtained from the Multi-resolution Emission
184   Inventory for China (MEIC), which has been compiled and maintained by Tsinghua University
185   since 2010 (Zheng et al., 2018; Wang et al., 2014). CO_2 emissions and boundary conditions were
186   derived from the NOAA CarbonTracker CT2019 dataset (Jacobs et al., 2021). The initial
187   meteorological boundary data, such as temperature, relative humidity, and wind, are derived
188   from the ERA-Interim reanalysis dataset with a horizontal resolution of 0.125°, a temporal
189   resolution of 6 hours, and 37 vertical levels (Liu et al., 2018b). The weekly mean Sea Surface
190   Temperature dataset was obtained from the National Ocean and Atmosphere Administration
191   (NOAA) (Reynolds et al., 2002).

192   The simulation domain was illustrated in Figure 1, with the target region centered at 36°N
193   and 107°E, and a grid resolution of 60 km by 60 km. The model used 18 vertical levels, ranging
194   from the surface to 50 hPa.

195   In the Base experiment, we incorporated interannual variations in anthropogenic emissions,
196   meteorological fields, and CO_2 emissions. Meteorological conditions (CO_2 emissions) were kept
197   constant at 2008 levels over ten years, referred to as the $SIM_{MET=2008}$ ($SIM_{CO2=2008}$) experiment.

198   The changes in O_3 concentrations relative to 2008 between 2009 and 2018 were determined
199   by comparing simulations of different years with 2008 in the Base experiment (Eq. (1)). The
200   impact of changed meteorological conditions on O_3 concentrations relative to 2008 was assessed
201   by comparing results between $SIM_{MET=2008}$ and the Base experiment in the same year (Eq. (2)).
202   The contribution of changed CO_2 emissions was similarly estimated (Eq. (3)). Finally, the
203   influence of anthropogenic emissions was calculated by excluding the impact of meteorological
204   factors and CO_2 from the changes in O_3 concentrations (Eq. (4)). Table 1 shows the results of the
205   numerical experiments.

206    $\Delta O_i = Base_i - Base_{2008}$ (1)
207
208    $\Delta M_i = Base_i - SIM_{i,MET=2008}$ (2)
209
210    $\Delta C_i = Base_i - SIM_{i,CO2=2008}$ (3)
211
212    $\Delta E_i = \Delta O_i - \Delta M_i - \Delta C_i$ (4)
213    $\triangle O_i$: The changes in O_3 concentrations in the year i relative to 2008.
214    $Base_i$: The O_3 concentrations in the Base experiment in the year i.

215 ΔM_i : The changes in O_3 concentrations in the year i due to meteorological factors variations.

216 $SIM_{i,MET=2008}$: The O_3 concentrations in the $SIM_{MET=2008}$ experiment in the year i.

217 ΔC_i : The changes in O_3 concentrations in the year i due to CO_2 variations.

218 $SIM_{i,CO2=2008}$: The O_3 concentrations in the $SIM_{CO2=2008}$ experiment in the year i.

219 ΔE_i : The changes in O_3 concentrations in the year i due to anthropogenic emissions variations.

220 **Table 1.** The Numerical experimental in this study.

Experiment	Time	Meteorological fields	CO_2 emissions	Anthropogenic emissions
Base	2008-2018	Varying	Varying	Varying
$SIM_{MET=2008}$	2009-2018	2008	Varying	Varying
$SIM_{CO2=2008}$		Varying	2008	Varying

221

222 In this work, both meteorological and CO_2 boundary conditions were kept consistent in base
223 and sensitivity studies. We did not consider the impact of boundary conditions on O_3 due to the
224 following reasons. First, in general, the regional model was coupled with the global model to get
225 a more realistic influence from the boundary. However, for long-term climate-chemistry
226 modeling, the such coupling means a large computing resource. Second, the boundary conditions
227 were derived from global models (Liu et al., 2017; Ban et al., 2014) and have to be prescribed in
228 sensitive experiments. Finally, fixed boundary conditions were widely used in some O_3 studies in
229 China (Liu and Wang, 2020a, b; Wang et al., 2019b). Moreover, regional emissions are the
230 primary source of surface O_3 in China, with contributions accounting for 80% from May to
231 August (Lu et al., 2019). Therefore, the impact of fixed boundary conditions can be ignored in
232 the current stage.

233 **3 Results and discussion**

234 3.1 Model evaluation

235 The ability of RegCM to reproduce East Asian climate and air quality has been widely evaluated
236 in recent years. Previous studies have demonstrated that RegCM was capable of the essential
237 characteristics and interannual variations of air components and meteorological fields in East
238 Asia(Xu et al., 2022b; Ma et al., 2023; Zhuang et al., 2018). Given that the monitoring of near-
239 surface O_3 levels by CNEMC was initiated only in late 2013, the monitoring sites in 2013 and
240 2014 were limited, and the monitoring period was disjointed. As a result, in this study, we
241 compared the simulated meteorological fields, O_3, and CO_2 levels with observations only from
242 2015 to 2018.

243 Figures S1~4 demonstrated that the RegCM-Chem-YIBs model effectively captured the
244 spatial distribution and magnitude of temperature, humidity, and wind over East Asia at 500 hPa,
245 850 hPa, and 1000 hPa between 2015 and 2018. However, due to the complex terrain's influence
246 on the lower atmosphere, most models show better results at higher levels (Zhuang et al., 2018;
247 Anwar et al., 2019; Xie et al., 2019). Thus, the simulations at 500 hPa were more consistent with
248 the reanalysis data. At 1000 hPa, the simulated wind speed was slightly higher than the
249 reanalysis data in eastern China. This difference may be due to common deficiencies in

250 meteorological models, such as insufficient horizontal resolution, initial and boundary conditions,
251 and physical parameterizations(Cassola and Burlando, 2012; Accadia et al., 2007), particularly in
252 areas with low wind speeds (Carvalho et al., 2012).

253   Figures S5 and S6 demonstrated that the model accurately reproduced the observed increase
254 in surface CO_2 and O_3 from 2015 to 2018, with high correlation coefficients ranging from 0.39 to
255 0.74 (Table 2). The model effectively captured the high concentrations of O_3 in major urban
256 areas such as the NCP, the YRD, the PRD, the SCB, and the FWP, while also successfully
257 reproducing the gradient in CO_2 concentrations between eastern and western China. However,
258 the model slightly underpredicted MDA8 O_3 concentrations (-4.02 to -3.21 ppb) and
259 overestimated CO_2 levels (3.32~7.07 ppm). These discrepancies are mainly attributed to
260 uncertainties in the emissions inventory (Hong et al., 2017). Overall, the simulated
261 meteorological factors and surface CO_2 and O_3 concentrations were deemed acceptable.
262
263 **Table 2.** Evaluations of the surface CO_2 (units: ppm) and MDA8 O_3 (units: ppb) during the summer
264 monsoon period in East Asia.

Species	Year	OBS	SIM	MB	RMSE	R
CO_2(ppm)	2015	402.82	406.98	4.16	9.37	0.44
	2016	407.12	410.44	3.32	8.22	0.69
	2017	408.35	413.62	5.27	11	0.39
	2018	409.61	416.68	7.07	11.32	0.41
MDA8 O_3(ppb)	2015	48.77	44.75	-4.02	29.39	0.57
	2016	50.16	46.95	-3.21	27.56	0.60
	2017	55.43	51.87	-3.56	21.55	0.74
	2018	55.53	52.08	-3.42	24.78	0.73

265 OBS: observation; SIM: simulation; MB: bias; NMB: normalized mean bias; RMSE: root mean square
266 error; R: correlation coefficient. MDA8 O_3: the maximum daily 8-hour average O_3.

267 3.2 Ozone variation from 2008 to 2018

268 Figure S7 illustrates the mean seasonal MDA8 O_3 concentrations in East Asia during the summer
269 monsoon period from 2008 to 2018. High O_3 concentrations appeared in eastern China, which
270 can be attributed to increased emissions, high temperatures, humidities, and intense radiation in
271 the region (Gao et al., 2020; Mousavinezhad et al., 2021; Wei et al., 2022). Surface O_3 increased
272 annually in most of China between 2008 to 2018, with megacity clusters experiencing a more
273 significant increase.

274   We conducted a regional analysis of surface O_3 increases in five target regions: the NCP,
275 the YRD, the PRD, the SCB, and the FWP. In 2018, the surface MDA8 O_3 concentrations
276 averaged 74 ppb in the NCP region, while the other areas had lower concentrations (ranging
277 from 42 to 67 ppb in the FWP, YRD, PRD, and SCB). The lower surface O_3 levels in the SCB
278 and FWP regions were attributed to lower anthropogenic emissions. The YRD and PRD regions
279 were more affected by meteorological factors, with the East Asian summer monsoon bringing in
280 cleaner air and precipitation from the sea, leading to lower air pollution concentrations (He et al.,
281 2012). The spatial distribution and increasing trend of surface MDA8 O_3 concentrations in China
282 were consistent with previous studies (Li et al., 2020; Shen et al., 2022).

283   Figure 2 and Table 3 illustrate the changes in surface MDA8 O_3 concentrations from 2009
284 to 2018 relative to 2008. The surface MDA8 O_3 concentrations in China increased drastically
285 over the past decade, particularly in 2017 and 2018 (6.79~32.03 ppb). We divided the period

from 2009 to 2018 into two phases based on the Clean Air Action Plan implemented in 2013: the pre-governance period (PreG, 2009~2013) and the post-governance period (PostG, 2014~2018). The surface MDA8 O_3 concentration increased significantly in NCP (18.42 ppb), followed by SCB (11.21 ppb), FWP (10.9 ppb), and the YRD (10.07 ppb), while increased slightly in PRD (4.94 ppb), in PosG relative to 2008. Our results were consistent with previous studies by Lu et al. (2020), Ma et al. (2016), and Mousavinezhad et al. (2021).
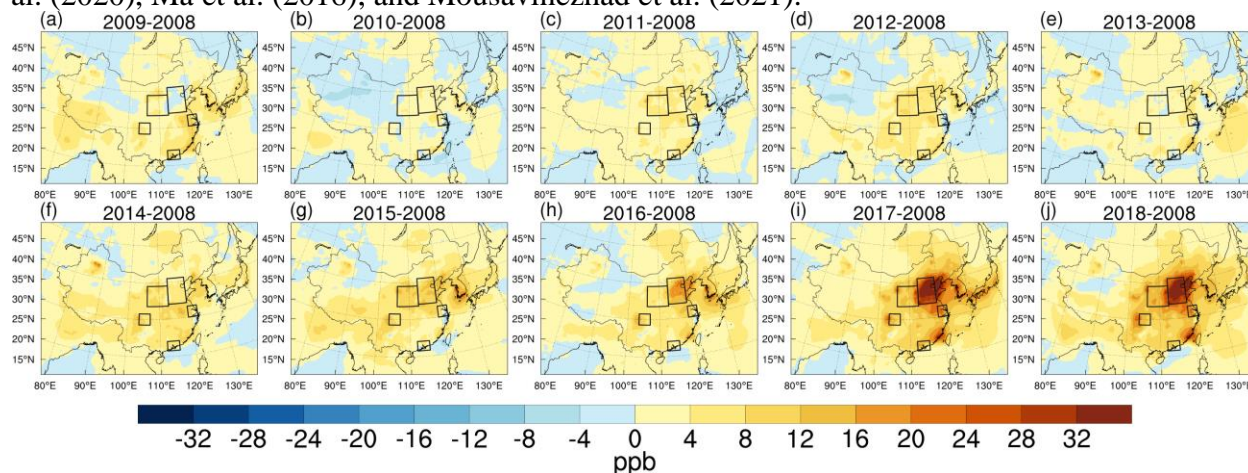
Figure 2. Changes in the surface MDA8 O_3 concentrations (units: ppb) during the summer monsoon period from 2009 (a), 2010 (b), 2011 (c), 2012 (d), 2013 (e), 2014 (f), 2015 (g), 2016 (h), 2017 (i) and 2018 (j) relative to 2008.

Table 3. The changes of MDA8 O_3 over North China Plain, Fenwei Plain, Yangtze River Delta, Pearl River Delta, and Sichuan Basin during the summer monsoon period from 2009 to 2018 relative to 2008.

Regions	2009	2010	2011	2012	2013	2014	2015	2016	2017	2018	PreG	PostG
NCP	0.14	2.85	4.53	6.13	2.7	4.78	10.1	14.25	30.92	32.03	3.27	18.42
FWP	3.23	1.78	5.01	6.78	1.37	7.9	10.5	6.24	13.71	16.17	3.63	10.90
YRD	8.33	1.47	1.46	0.5	3.12	6.04	3.46	7.09	17.64	16.12	2.98	10.07
PRD	5.76	-0.26	2.56	5.13	-0.4	3.82	1.46	3.16	9.45	6.79	2.56	4.94
SCB	4.92	1.03	3.46	5	3.94	8.54	9.27	9.78	13.67	14.8	3.67	11.21

3.3 The effect of meteorology in 2008~2018 ozone increase

Overall, the meteorological variations from 2008 to 2018 were unfavorable for the O_3 increase during the EASM period, as illustrated in Figure 3.

Based on Figure 3 and Table 4, it is evident that meteorological conditions had a significant impact on surface MDA8 O_3 in the NCP and FWP regions during the PostG period (-0.09~-0.04 ppb) compared to the PreG period (-1.41~-0.88 ppb). In the SCB region, the impact of meteorological fields was relatively weak (-0.41~0.71 ppb), attributed to the basin topography and stable atmospheric conditions. However, in the eastern and southeastern coastal areas of China, due to the significant influence of the EASM, the impact of meteorological conditions may be more critical than that of anthropogenic emissions. For instance, in the YRD and PRD regions, meteorological conditions significantly changed O_3 levels (-1.29~1.3 ppb) compared to anthropogenic emissions (0.81~0.87 ppb) in 2013, indicating the significant influence of meteorological conditions on surface O_3.

Our findings are consistent with previous studies. Liu and Wang (2020a) reported a decrease

313 in O$_3$ in Shanghai from 2013 to 2017 due to changes in meteorological conditions. Chen et al.
314 (2019) and Liu and Wang (2020a) also suggested that changed meteorological conditions had a
315 negative impact on O$_3$ formation in the NCP and FWP regions, and that the influence of
316 meteorology on surface-level O$_3$ decreased in PostG. In addition, Cheng et al. (2019) found that
317 the effects of meteorological conditions on long-term O$_3$ variations were less than 3%, which is
318 similar to our study.

319 As we know, the formation of surface O$_3$ is promoted by rising temperatures (Steiner et al.,
320 2010). However, increased surface temperatures can also intensify turbulence within the
321 planetary boundary layer (PBL), increasing PBL height (Guo et al., 2016). This increase in PBL
322 height, coupled with the enhanced upward motion, can transport near-surface pollutants to the
323 upper atmosphere, reducing their concentration in the lower atmosphere (Gao et al., 2016).
324 Additionally, the upward motion can also facilitate cloud formation and precipitation, resulting in
325 a reduction of near-surface atmospheric pollutants via precipitation washout (Yoo et al., 2014).

326 We have improved the accuracy of O$_3$ photodissociation rate calculations by including
327 varying AOD and SSA in the TUV module, as described in Section 2.3.2. As a result, the
328 increase in cloud cover reduced the shortwave radiation flux and photochemical formation rates
329 of near-surface O$_3$, leading to decreased formation. Thus, the increase in near-surface
330 temperature is often accompanied by an elevation in PBL height, enhanced cloud cover,
331 precipitation, and reduced shortwave radiation. Moreover, higher wind speeds can enhance the
332 dispersion of O$_3$ (Gorai et al., 2015).

333 The variations of MDA8 O$_3$, precipitation, clouds, shortwave flux (SWF), wind speed,
334 temperature, and PBL height are presented individually in Figure 4. The increase in SWF can
335 accelerate O$_3$ formation through photochemistry (Jiang et al., 2012; Lelieveld and Crutzen, 1990).
336 Therefore, the increased cloud fraction reduced surface O$_3$ by decreasing shortwave radiation,
337 especially in NCP, FWP, YRD, and SCB in the PreG period (-10.63~-1.6 W/m^2). Furthermore,
338 the enhanced precipitation in these regions (0.37~1.81 mm/day) reduced surface O$_3$ levels
339 significantly. The significant increase in wind speed (0.17~0.26 m/s) also contributed to the
340 reduction of surface O$_3$ in the NCP region (Table 4).

341 Another crucial factor is the elevated surface temperature (0~5 K), which intensified
342 upward motion and raised the planetary boundary layer (PBL) height (0~500 m) across much of
343 East Asia. Consequently, the increased temperature and PBL height could disperse surface-level
344 O$_3$, thereby reducing its concentration.
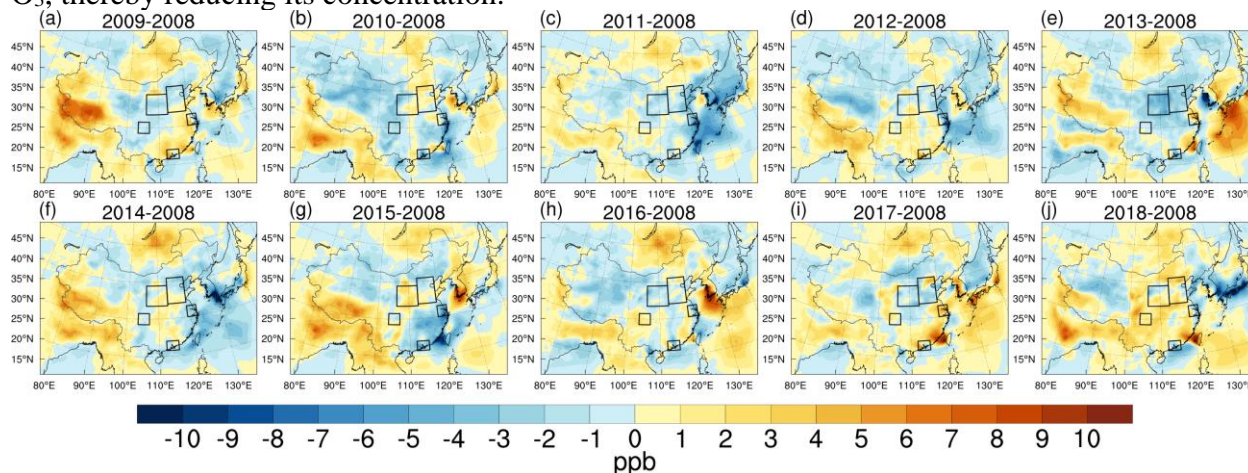
345

346 **Figure 3.** The responds of the surface MDA8 O_3 mixing ratios (units: ppb) to variations in meteorological
347 conditions during the summer monsoon period in 2009 (a), 2010 (b), 2011 (c), 2012 (d), 2013 (e), 2014
348 (f), 2015 (g), 2016 (h), 2017 (i) and 2018 (j) relative to 2008.
349

350

351

352

353

354

355
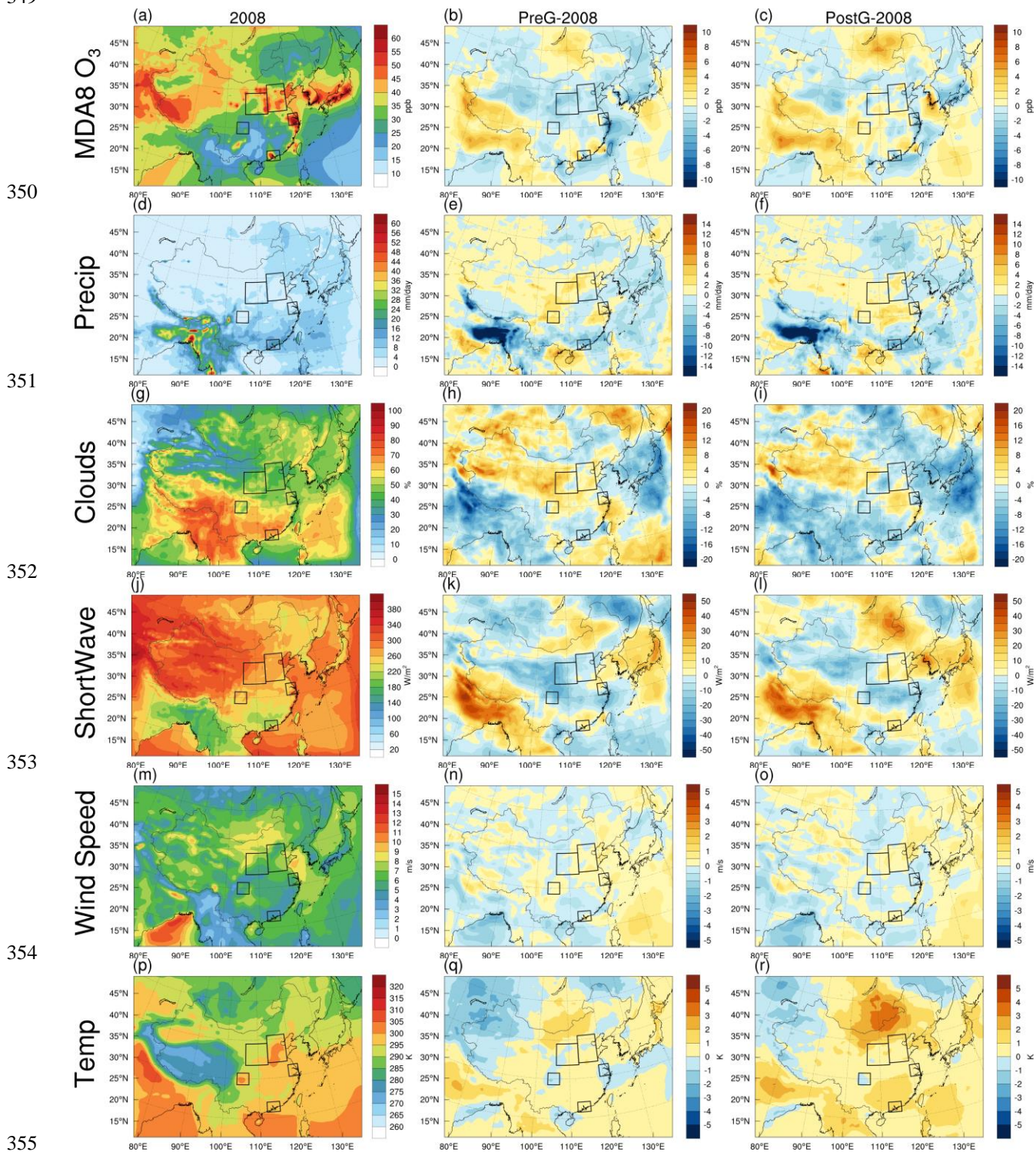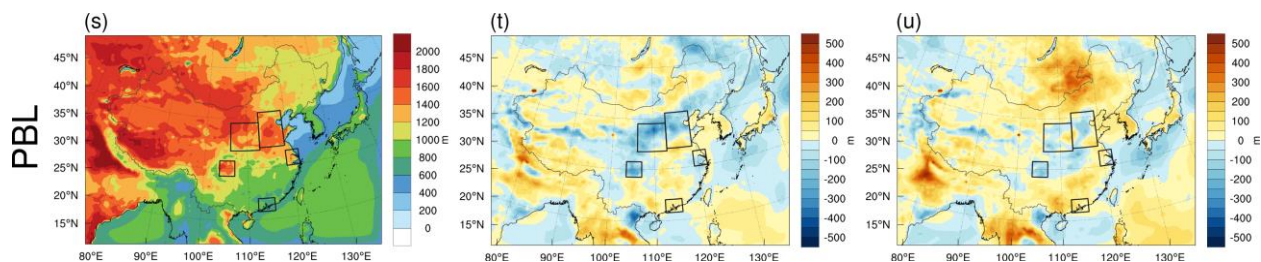
Figure 4. The MDA8 O_3 (a~c, units: ppb), precipitation (d~f, units: mm/day), clouds (g~i, units: %), shortwave flux (j~l, units: W/m^2), wind speed (m~o, units: m/s), temperature (p~r, units: K), and planetary boundary layer height (s~u, units: m) during the summer monsoon period in 2008 from the base simulations (the left column) and their responses due to variations in meteorological conditions in PreG (2009~2013, the central column) and PostG (2014~2018, the right column) relative to 2008.

Table 4. Response of the MDA8 O_3 mixing ratios (units: ppb), precipitations (units: mm/day), clouds fraction (units: %), shortwave flux (units: W/m^2), wind speed (units: m/s), temperature (units: K), and planetary boundary layer height (units: m) to the changes in meteorological conditions over North China Plain, Fenwei Plain, Yangtze River Delta, Pearl River Delta, and Sichuan Basin during the summer monsoon period in PreG (2009~2013) and PostG (2014~2018) relative to 2008.

Regions	Period	MDA8 O_3 (ppb)	Precip (mm/day)	Clouds (%)	SWF (W/m^2)	Wind Speed (m/s)	Temp (K)	PBL (m)
NCP	PreG	-0.88	0.58	1.33	-3.04	0.17	0.32	-46.8
	PostG	-0.04	0.6	-0.93	3.06	0.26	0.6	-14.5
FWP	PreG	-1.41	1.68	2.86	-10.63	-0.06	0.1	-108.5
	PostG	-0.09	0.81	-0.94	-0.81	0.05	0.46	-15.3
YRD	PreG	-1.03	1.02	1.07	-1.6	0.18	-0.29	-33.9
	PostG	-0.96	0.48	-1.18	-4.85	-0.08	0.45	21.9
PRD	PreG	-0.23	-2.39	-1.93	2.24	-0.02	0.36	29.6
	PostG	-1.08	-3.24	-3.98	5.37	0.18	1.00	52.2
SCB	PreG	-0.41	1.81	0.59	-8.8	0.13	-0.58	-136.5
	PostG	0.71	0.37	-2.23	-3.2	-0.03	-0.14	-76

3.4 The effect of CO_2 in 2008~2018 ozone increase

The surface O_3 in southern China, which includes the YRD, PRD, and SCB regions, was characterized by high precipitation, temperatures, and vegetation cover, and was significantly impacted by CO_2 (Figure 5). Figures 6 e and f demonstrate a marked rise in CO_2 levels across East Asia, particularly in eastern China, which was attributable to extensive human activity.

CO_2 is a significant driver of climate change and alterations in biogenic emissions. As shown in Figures 6 b and c, the impact of CO_2 on O_3 levels varies across locations, with a positive effect of 0.28~0.46 ppb along the southeastern coast of China but a negative influence of -0.51 to -0.11 ppb in the southwest and central China. CO_2 affects O_3 concentration by influencing both precipitation and isoprene emissions. In western and central China, CO_2 primarily affects O_3 concentration through its impact on precipitation (Table 5). Elevated CO_2 concentrations lead to increased precipitation (0.06~0.64 mm/day) in the FWP and SCB regions, resulting in a decrease in surface O_3 (up to -0.51 ppb). In eastern and southern coastal China, where vegetation is abundant, CO_2 has a greater impact on isoprene emissions. In the YRD region, decreased isoprene (-0.58 to -0.32 μg/m^3) and increased precipitations (0.09~0.13

mm/day) reduced MDA8 O_3 levels (0.09~0.14 ppb). In PRD, increased isoprene levels (0.31~0.92 μg/m^3) and decreased precipitations (-1.02~-0.33 mm/day) led to the enhancement of MDA8 O_3 (0.28~0.46 ppb).

In some years, the impact of changed CO_2 can be as significant as or even surpass that of anthropogenic emissions and meteorology (Figure 10). For example, in 2013, CO_2 caused an increase of 0.95 ppb in MDA8 O_3 in the YRD region, which exceeded that of anthropogenic emissions (0.87 ppb). Similarly, in the PRD region in 2012, the effect of CO_2, anthropogenic emissions, and meteorology was 1.41, 1.77, and 1.95 ppb, respectively. Even in the NCP in 2010, the impact of CO_2 (0.75 ppb) was comparable to that of anthropogenic emissions (1.5 ppb). In summary, CO_2 has a significant impact on surface O_3 concentrations by influencing radiation and isoprene emissions, with more prominent effects in regions with abundant vegetation.
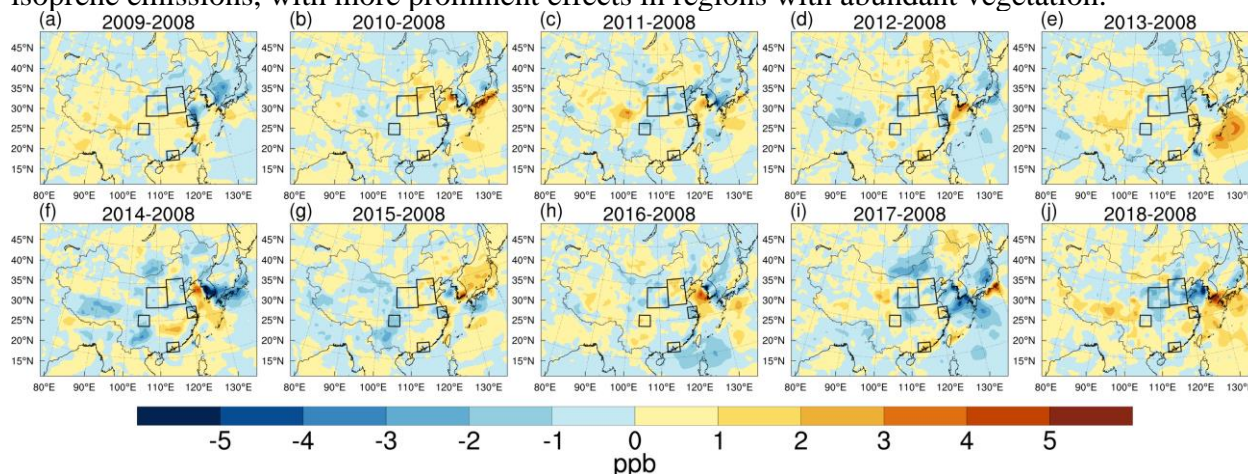
Figure 5. Simulated responses of surface MDA8 O_3 mixing ratios (units: ppb) to the variations in CO_2 emissions during the summer monsoon period in 2009 (a), 2010 (b), 2011 (c), 2012 (d), 2013 I, 2014 (f), 2015 (g), 2016 (h), 2017 (i) and 2018 (j) relative to 2008.
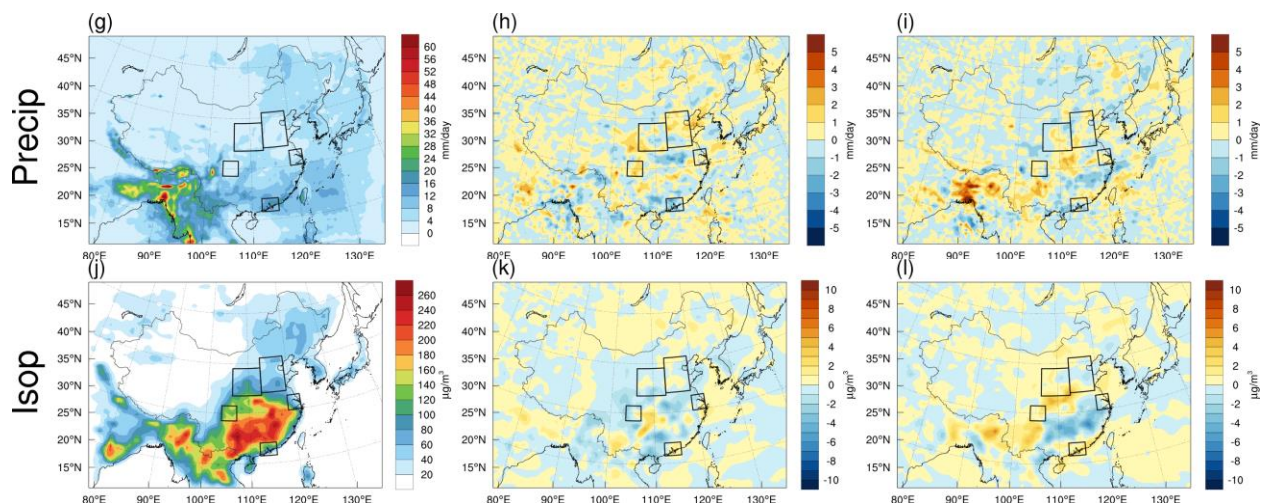
Figure 6. The simulated averaged MDA8 O_3 (a~c, units: ppb), CO_2 (d~f, units: ppm), precipitation (g~i, units: mm/day), and isoprene mixing ratios (j~l, units: μg/m^3) in 2008 from the base simulations (the left column) and their changes due to variations in CO_2 emissions in PreG (2009~2013, the central column) and PostG (2014~2018, the right column) relative to 2008.

Table 5. Simulated responses of MDA8 O_3 mixing ratios (units: ppb), CO_2 mixing ratios (units: ppm), precipitations (units: mm/day), and isoprene mixing ratios to the changes in CO_2 emissions over North China Plain, Fenwei Plain, Yangtze River Delta, Pearl River Delta, and Sichuan Basin in PreG (2009~2013) and PostG (2014~2018) relative to 2008.

Regions	Period	MDA8 O_3 (ppb)	CO_2 (ppm)	Precipitation (mm/day)	Isoprene (μg/m^3)
NCP	PreG	0.07	3.19	0.27	-0.1
	PostG	-0.05	4.24	0.13	0.26
FWP	PreG	-0.11	1.70	0.21	-0.16
	PostG	-0.51	2.05	0.06	0.33
YRD	PreG	-0.09	4.1	0.13	-0.32
	PostG	-0.14	6.2	0.09	-0.58
PRD	PreG	0.46	1.97	-1.02	0.31
	PostG	0.28	3.20	-0.33	0.92
SCB	PreG	-0.30	2.80	0.64	-0.78
	PostG	-0.30	2.78	0.21	0.69

3.5 The effect of anthropogenic emission in 2008~2018 ozone increase

Finally, we calculated the anthropogenic emissions' effect on the 2008~2018 O_3 increase. Figure S8 and Table S1 illustrate that the levels of PM$_{2.5}$, PM$_{10}$, SO$_2$, CO, and OC emissions remained consistently high during the PreG period. However, a linear decrease in emissions was observed after the implementation of the Clean Air Action Plan in 2013. Prior to 2013, the emission of VOCs increased steadily but subsequently stabilized. Similarly, the emission of nitrogen oxides (NOx) exhibited an upward trend before 2013, but since then, the emissions have shown a linear decrease, with each subsequent year exhibiting lower levels of NOx emissions. In comparison to other species, the emissions of ammonia (NH$_3$) remained relatively stable from 2008 to 2018. Our analysis results of the emissions of different species align with those of Zheng et al. (2018), who computed the changes of each species in the MEIC inventory from 2010 to 2017.

Figure 7 illustrates that anthropogenic emissions have caused a notable increase in surface

424 O_3 levels across most of China, particularly in megacity clusters. The impact of anthropogenic
425 emissions on O_3 concentration ranged from 2.33 to 18.51 ppb in the five target regions.

426   Figure 8 and Table 6 illustrate that the changes in surface O_3 caused by anthropogenic
427 emissions are similar in magnitude and spatial distribution to the changes in the base experiment.
428 This suggests that anthropogenic emissions were the dominant factor driving the increase of
429 surface O_3 in China from 2008 to 2018. Notably, a high-impact center of anthropogenic
430 emissions was simulated in North China, with the NCP region experiencing the most significant
431 increase in surface O_3 (4.08~18.51 ppb), followed by the FWP, YRD, and SCB regions
432 (4.10~11.5 ppb). In the PRD region, anthropogenic emissions led to a slight enhancement of O_3
433 by 2.33~5.74 ppb.

434   The role of anthropogenic emissions increased linearly from 2008 to 2018, despite the
435 implementation of the Clean Air Action Plan in 2013 (Table 6). For example, anthropogenic
436 emissions significantly increased surface MDA8 O_3 in the NCP region (4.08 ppb in PreG and
437 18.51 ppb in PostG). Similarly, FWP experienced increases of 5.15 and 11.5 ppb in the PreG and
438 PostG periods, respectively. In the SCB region, the surface MDA8 O_3 was mainly affected by
439 variations in anthropogenic emissions due to the high levels of anthropogenic emissions in the
440 complex basin topography. In the YRD and PRD regions, anthropogenic emissions resulted in
441 changes to O_3 of 2.56~10.07 ppb.

442   The reasons for this characteristic are multiple. Before 2013, the continuous increase in
443 VOCs and NOx emissions (Figure S8 b, c) facilitated the rise of O_3 levels. Following the
444 implementation of the Clean Air Action Plan in 2013, the emissions of VOCs and NOx were
445 regulated. However, with the decrease in $PM_{2.5}$ levels, direct radiation increased, and scattered
446 radiation decreased (Figure 9), thereby promoting the photochemical formation of O_3 (Bian et al.,
447 2007). In addition, the reduced NO emission weakened the titration effect (Figure S8 b), thus
448 increasing surface O_3 (Li et al., 2022).
449   Our results are consistent with previous studies by Wang et al. (2019b) and Liu and Wang
450 (2020b), which also showed the dominant and almost linear role of anthropogenic emissions in
451 the increase of O_3 from 2013 to 2015 in four major Chinese cities (Beijing, Shanghai,
452 Guangzhou, and Chengdu).
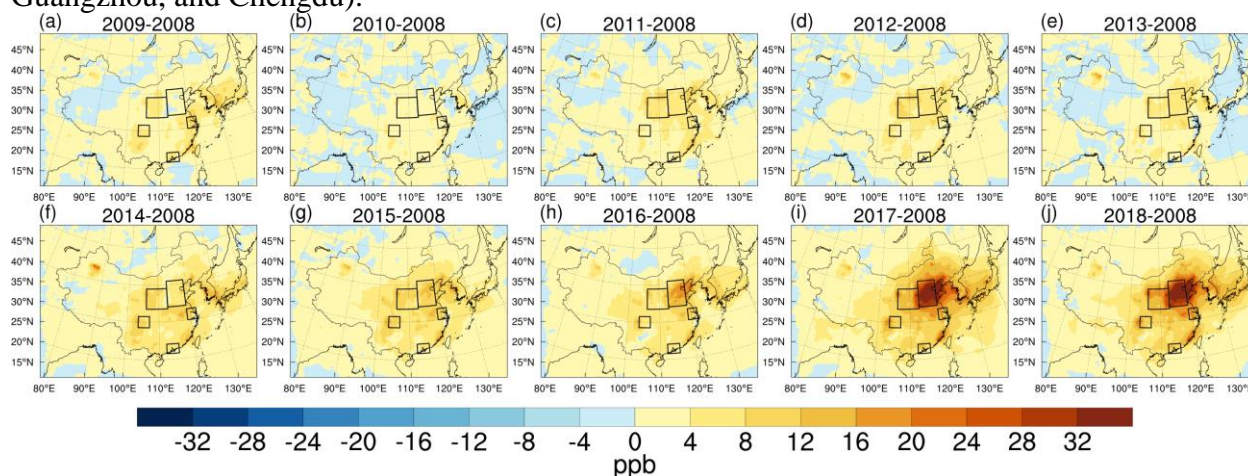
453
454 **Figure 7.** Simulated responses of the surface MDA8 O_3 mixing ratios (units: ppb) to variations in
455 anthropogenic emissions in 2009 (a), 2010 (b), 2011 (c), 2012 (d), 2013 (e), 2014 (f), 2015 (g), 2016 (h),
456 2017 (i) and 2018 (j) relative to 2008.
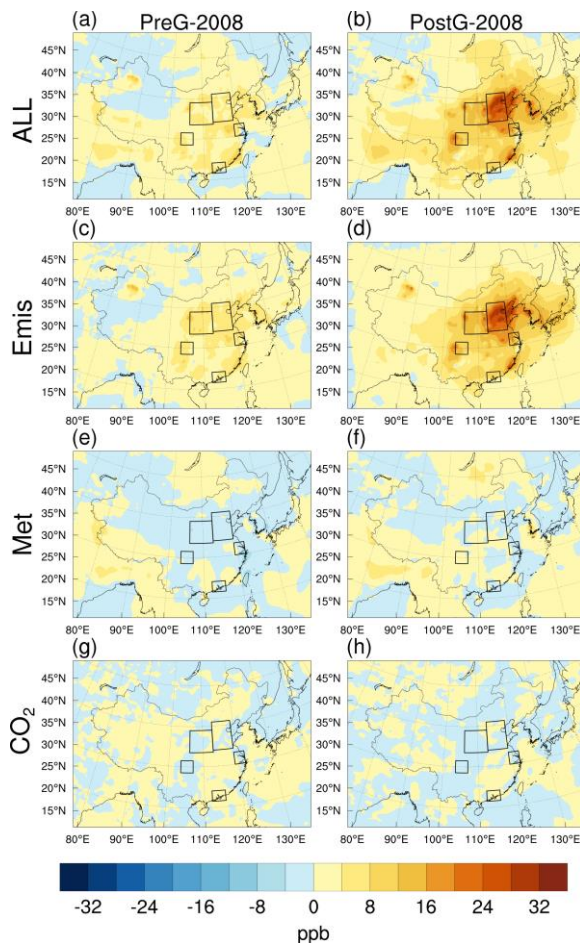
457
Figure 8. Changes in the simulated surface MDA8 O_3 mixing ratios (units: ppb) from the base simulation
459 (All, a,b); those due to variations in anthropogenic emissions (Emis, c,d), meteorological conditions (Met,
460 e,f), and CO_2 emissions (CO_2, g,h) in PreG (2009~2013, the left column) and PostG (2014~2018, the
461 right column) relative to 2008.
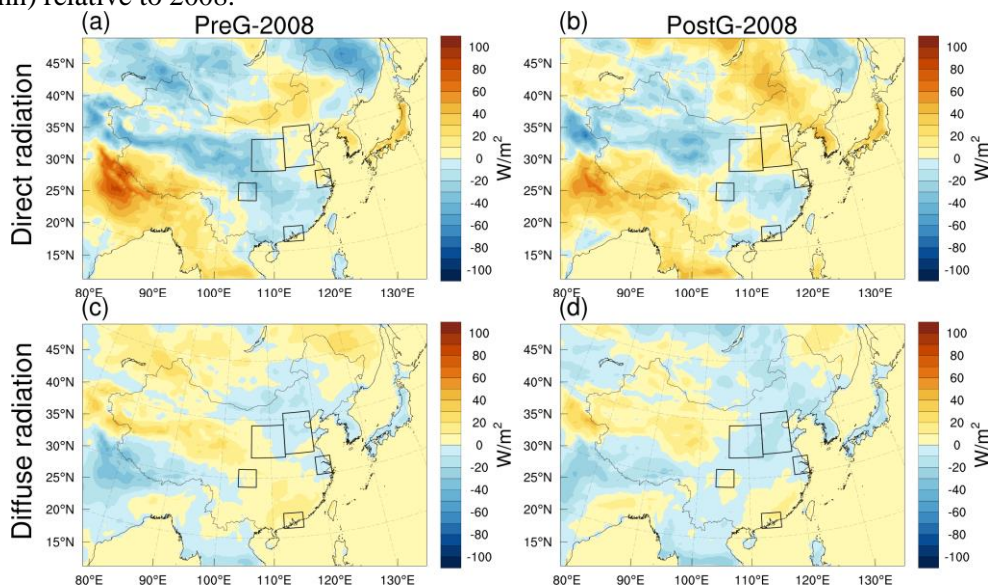
463
Figure 9. The variations of the surface direct radiation (a,b, units: W/m^2) and diffuse radiation (c,d, units:
465 W/m^2) in the PreG (2009~2013, a,c) and PostG (2014~2018, b,d) period relative to 2008.

466

Table 6. Simulated response of the MDA8 O_3 mixing ratios (units: ppb) to the changes in anthropogenic emissions (Emis), meteorological conditions (Met), and CO_2 emissions (CO_2) over North China Plain, Fenwei Plain, Yangtze River Delta, Pearl River Delta, and Sichuan Basin in PreG (2009~2013) and PostG (2014~2018) relative to 2008.

Regions	Period	ALL (ppb)	Emis (ppb)	Met (ppb)	CO_2 (ppb)
NCP	PreG	3.27	4.08	-0.88	0.07
	PostG	18.42	18.51	-0.04	-0.05
FWP	PreG	3.63	5.15	-1.41	-0.11
	PostG	10.9	11.5	-0.09	-0.51
YRD	PreG	2.98	4.10	-1.03	-0.09
	PostG	10.07	11.17	-0.96	-0.14
PRD	PreG	2.56	2.33	-0.23	0.46
	PostG	4.94	5.74	-1.08	0.28
SCB	PreG	3.67	4.38	-0.41	-0.30
	PostG	11.21	10.80	0.71	-0.30

3.6 Attribution analysis of ozone changes in 2008~2018

Finally, we presented an attribution diagram depicting the changes in O_3 concentration from 2008 to 2018. The total variation in O_3 concentration can be attributed to the combined effects of meteorological changes, changes in CO_2 concentration, and anthropogenic emissions (Figure 10).

The primary driver of the O_3 concentration variation from 2008 to 2018 was the changes in anthropogenic emissions, particularly in regions with high emissions, such as the NCP and FWP. Although the Clean Air Action Plan was implemented in 2013, it did not reduce the contribution of anthropogenic emissions to the O_3 increase. Even in the PostG period, with the development of urbanization and industrialization, the impact of changed anthropogenic emissions on O_3 has gradually become more prominent than changed meteorology and CO_2. The contribution of changed meteorology to O_3 was generally negative in the five regions, with a more significant impact in the YRD and PRD regions. This may be attributed to their proximity to the ocean and susceptibility to the summer monsoon influence. Changes in CO_2 concentration affected O_3 concentration by altering radiation and isoprene emissions, with a more significant impact in the YRD and PRD regions where vegetation was abundant. In some years, it even surpassed the effects of anthropogenic emissions. Therefore, we suggest that the influence of CO_2 concentration changes on O_3 concentration should be considered in regions with high vegetation coverage.

489
490
491
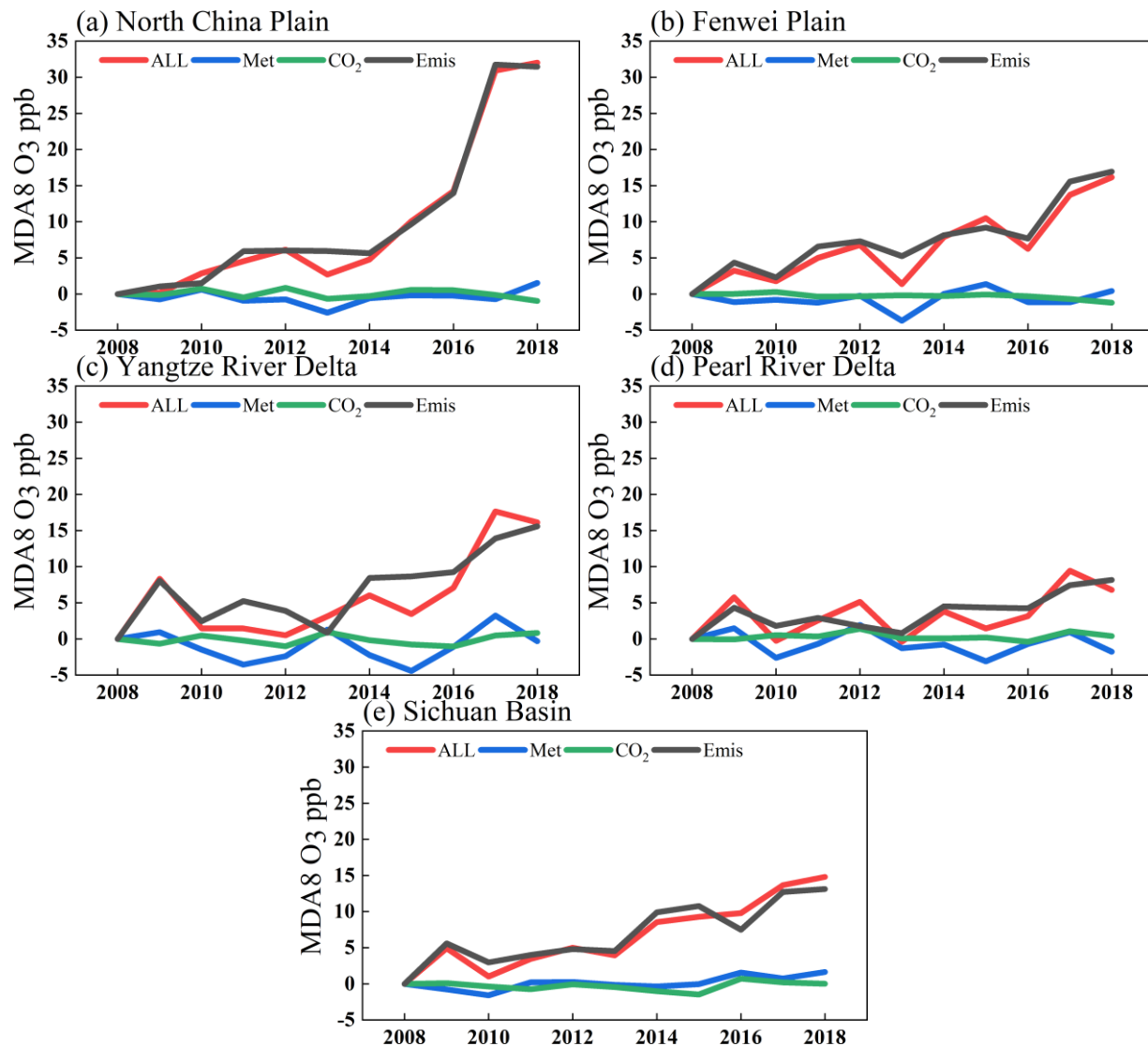
Figure 10. Interannual variations of the surface MDA8 O_3 mixing ratios (units: ppb) in the summer monsoon period (ALL) and the responses of variations in anthropogenic emissions (Emis), meteorological conditions (Met), and CO_2 emissions (CO_2) in (a) North China Plain, (b) Fenwei Plain, (c) Yangtze River Delta, (d) Pearl River Delta, and (e) Sichuan Basin in 2008~2018 relative to 2008.

4 Conclusions

In this study. First, we improved the RegCM-Chem-YIBs model regarding the photolysis of O_3 and the radiation effect of CO_2 and O_3. Second, we assessed the impacts of anthropogenic emissions, meteorological factors, and CO_2 on the surface O_3 increase in China during the EASM season from 2008 to 2018.

In the NCP and FWP regions. The increased surface O_3 (4.08~5.15 ppb in PreG and 11.5~18.51 ppb in PostG) was primarily attributed to the changes in anthropogenic emissions. Furthermore, the impact of anthropogenic emissions has increased linearly, despite the Clean Air Action Plan being implemented in 2013. In contrast, the effects of meteorological factors and CO_2 on O_3 were weak during the study period.

506   In the YRD and PRD regions. Ignoring the principal contributions of anthropogenic
507 emissions, CO_2 significantly impacted the O_3 variations (-0.14~0.46 ppb). The varied CO_2 led to
508 surface MDA8 O_3 changes of -0.09~-0.14 ppb in the YRD and 0.28~0.46 ppb in the PRD by
509 modulating the isoprene emissions and precipitations. On the other hand, the meteorological
510 conditions played a more significant role in surface O_3 than in NCP, FWP, and SCB regions,
511 resulting in a decrease in MDA8 O_3 from 2008 to 2018 (-4.42~3.25 ppb).

512   In the SCB region. The increase in surface O_3 from 2008 to 2018 was primarily driven by
513 variations in anthropogenic emissions. The effect of meteorological conditions was weak due to
514 the high level of emissions and basin topography. However, the changes in CO_2 significantly
515 impacted surface O_3 levels and were unfavorable to O_3 formation during the study period (-3.0
516 ppb in PreG and PostG).

517   In conclusion, anthropogenic emissions dominated the O_3 increase in China from 2008 to
518 2018, and the effects of meteorological conditions on surface O_3 could be more significant in
519 some regions. Furthermore, we emphasize the significance of CO_2 emissions, particularly in
520 southern China, as a critical contributor to O_3 variations. Therefore, it is vital to consider CO_2
521 variability in future predictions of O_3 concentrations. Such consideration would be helpful for
522 designing long-term O_3 control policies.
523

524 **Data availability**

525 ERA-Interim data are available at https://apps.ecmwf.int/datasets/data/interim-full-daily/.

526 MEICv1.3 data are available at http://meicmodel.org/?page_id=560. CarbonTracker data are

527 available at https://gml.noaa.gov/aftp/products/carbontracker/co2/CT2019/. OISST data are

528 available at https://downloads.psl.noaa.gov/Datasets/noaa.oisst.v2/. WDCGG CO_2 data are

529 available at https://gaw.kishou.go.jp/search/gas_species/co2/latest/. CNEMC data are available

530 at http://www.cnemc.cn/. only available in Chinese, last access 1 May 2022.

531

532 **Author contributions**
533   **DM:** performed experiments; **TW:** designed the overall research; **HW, YQ, JL, JaL, and**
534 **SL** reviewed and edited the manuscript; **BL, ML, and MX** contributed to the development of the
535 RegCM-Chem-YIBs model.

536

537 **Competing interests:**
538 The contact author has declared that none of the authors has any competing interests.
539

540 **Disclaimer**
541 Publisher's note: Copernicus Publications remains neutral with regard to jurisdictional claims in
542 published maps and institutional affiliations.
543

544 **Financial support**

545 This work was supported by the National Natural Science Foundation of China (42077192,
546 41621005), the National Key Basic Research & Development Program of China
547 (2020YFA0607802, 2019YFC0214603), Creative talent exchange program for foreign experts in
548 the Belt and Road countries, and the Emory University-Nanjing University Collaborative
549 Research Grant.

References

Accadia, C., Zecchetto, S., Lavagnini, A., and Speranza, A.: Comparison of 10-m wind forecasts from a regional area model and QuikSCAT Scatterometer wind observations over the Mediterranean Sea, Monthly Weather Review, 135, 1945-1960,https://doi.org/10.1175/mwr3370.1, 2007.

Anwar, S. A., Zakey, A. S., Robaa, S. M., and Wahab, M. M. A.: The influence of two land-surface hydrology schemes on the regional climate of Africa using the RegCM4 model (vol 136, pg 1535, 2019), Theoretical and Applied Climatology, 136, 1549-1550,https://doi.org/10.1007/s00704-018-2588-0, 2019.

Ashmore, M. R. and Bell, J. N. B.: THE ROLE OF OZONE IN GLOBAL CHANGE, Annals of Botany, 67, 39-48,https://doi.org/10.1093/oxfordjournals.aob.a088207, 1991.

Ballantyne, A. P., Alden, C. B., Miller, J. B., Tans, P. P., and White, J. W. C.: Increase in observed net carbon dioxide uptake by land and oceans during the past 50 years, Nature, 488, 70-+,https://doi.org/10.1038/nature11299, 2012.

Balsamo, G., Albergel, C., Beljaars, A., Boussetta, S., Brun, E., Cloke, H., Dee, D., Dutra, E., Munoz-Sabater, J., Pappenberger, F., de Rosnay, P., Stockdale, T., and Vitart, F.: ERA-Interim/Land: a global land surface reanalysis data set, Hydrology and Earth System Sciences, 19, 389-407,https://doi.org/10.5194/hess-19-389-2015, 2015.

Ban, N., Schmidli, J., and Schar, C.: Evaluation of the convection-resolving regional climate modeling approach in decade-long simulations, Journal of Geophysical Research-Atmospheres, 119,https://doi.org/10.1002/2014jd021478, 2014.

Bian, H., Han, S. Q., Tie, X. X., Sun, M. L., and Liu, A. X.: Evidence of impact of aerosols on surface ozone concentration in Tianjin, China, Atmospheric Environment, 41, 4672-4681,https://doi.org/10.1016/j.atmosenv.2007.03.041, 2007.

Borg, I., Groenen, P. J. F., Jehn, K. A., Bilsky, W., and Schwartz, S. H.: Embedding the Organizational Culture Profile Into Schwartz's Theory of Universals in Values, Journal of Personnel Psychology, 10, 1-12,https://doi.org/10.1027/1866-5888/a000028, 2011.

Carvalho, D., Rocha, A., Gomez-Gesteira, M., and Santos, C.: A sensitivity study of the WRF model in wind simulation for an area of high wind energy, Environmental Modelling & Software, 33, 23-34,https://doi.org/10.1016/j.envsoft.2012.01.019, 2012.

Cassola, F. and Burlando, M.: Wind speed and wind energy forecast through Kalman filtering of Numerical Weather Prediction model output, Applied Energy, 99, 154-166,https://doi.org/10.1016/j.apenergy.2012.03.054, 2012.

Chen, Z., Zhuang, Y., Xie, X., Chen, D., Cheng, N., Yang, L., and Li, R.: Understanding long-term variations of meteorological influences on ground ozone concentrations in Beijing During 2006-2016, Environmental Pollution, 245, 29-37,https://doi.org/10.1016/j.envpol.2018.10.117, 2019.

Cheng, N., Li, R., Xu, C., Chen, Z., Chen, D., Meng, F., Cheng, B., Ma, Z., Zhuang, Y., He, B., and Gao, B.: Ground ozone variations at an urban and a rural station in Beijing from 2006 to 2017: Trend, meteorological influences and formation regimes, Journal of Cleaner Production, 235, 11-20,https://doi.org/10.1016/j.jclepro.2019.06.204, 2019.

Collins, W. D., Bitz, C. M., Blackmon, M. L., Bonan, G. B., Bretherton, C. S., Carton, J. A., Chang, P., Doney, S. C., Hack, J. J., Henderson, T. B., Kiehl, J. T., Large, W. G., McKenna, D. S., Santer, B. D., and Smith, R. D.: The Community Climate System Model version 3 (CCSM3), Journal of Climate, 19, 2122-2143,https://doi.org/10.1175/jcli3761.1, 2006.

Dang, R., Liao, H., and Fu, Y.: Quantifying the anthropogenic and meteorological influences on summertime surface ozone in China over 2012-2017, Science of the Total Environment, 754,https://doi.org/10.1016/j.scitotenv.2020.142394, 2021.

Decker, M. and Zeng, X. B.: Impact of Modified Richards Equation on Global Soil Moisture Simulation in the Community Land Model (CLM3.5), Journal of Advances in Modeling Earth Systems, 1,https://doi.org/10.3894/james.2009.1.5, 2009.

Duan, X.-t., Cao, N.-w., Wang, X., Zhang, Y.-x., Liang, J.-s., Yang, S.-p., and Song, X.-y.: Characteristics Analysis of the Surface Ozone Concentration of China in 2015, Huanjing Kexue, 38, 4976-4982,https://doi.org/10.13227/j.hjkx.201703045, 2017.

Fang, Y., Fiore, A. M., Horowitz, L. W., Gnanadesikan, A., Held, I., Chen, G., Vecchi, G., and Levy, H.: The impacts of changing transport and precipitation on pollutant distributions in a future climate, Journal of Geophysical Research-Atmospheres, 116,https://doi.org/10.1029/2011jd015642, 2011.

Fiore, A. M., Levy, H., II, and Jaffe, D. A.: North American isoprene influence on intercontinental ozone pollution, Atmospheric Chemistry and Physics, 11, 1697-1710,https://doi.org/10.5194/acp-11-1697-2011, 2011.

Gao, M., Carmichael, G. R., Wang, Y., Saide, P. E., Yu, M., Xin, J., Liu, Z., and Wang, Z.: Modeling study of the 2010 regional haze event in the North China Plain, Atmospheric Chemistry and Physics, 16, 1673-1691,https://doi.org/10.5194/acp-16-1673-2016, 2016.

Gao, M., Gao, J., Zhu, B., Kumar, R., Lu, X., Song, S., Zhang, Y., Jia, B., Wang, P., Beig, G., Hu, J., Ying, Q., Zhang, H., Sherman, P., and McElroy, M. B.: Ozone pollution over China and India: seasonality and sources, Atmospheric Chemistry and Physics, 20, 4399-4414,https://doi.org/10.5194/acp-20-4399-2020, 2020.

Gauss, M., Myhre, G., Pitari, G., Prather, M. J., Isaksen, I. S. A., Berntsen, T. K., Brasseur, G. P., Dentener, F. J., Derwent, R. G., Hauglustaine, D. A., Horowitz, L. W., Jacob, D. J., Johnson, M., Law, K. S., Mickley, L. J., Muller, J. F., Plantevin, P. H., Pyle, J. A., Rogers, H. L., Stevenson, D. S., Sundet, J. K., van Weele, M., and Wild, O.: Radiative forcing in the 21st century due to ozone changes in the troposphere and the lower stratosphere, Journal of Geophysical Research-Atmospheres, 108,https://doi.org/10.1029/2002jd002624, 2003.

Giorgi, F. and Mearns, L. O.: Introduction to special section: Regional climate modeling revisited, Journal of Geophysical Research-Atmospheres, 104, 6335-6352,https://doi.org/10.1029/98jd02072, 1999.

Giorgi, F., Coppola, E., Solmon, F., Mariotti, L., Sylla, M. B., Bi, X., Elguindi, N., Diro, G. T., Nair, V., Giuliani, G., Turuncoglu, U. U., Cozzini, S., Guettler, I., O'Brien, T. A., Tawfik, A. B., Shalaby, A., Zakey, A. S., Steiner, A. L., Stordal, F., Sloan, L. C., and Brankovic, C.: RegCM4: model description and preliminary tests over multiple CORDEX domains, Climate Research, 52, 7-29,https://doi.org/10.3354/cr01018, 2012.

Gorai, A. K., Tuluri, F., Tchounwou, P. B., and Ambinakudige, S.: Influence of local meteorology and NO2 conditions on ground-level ozone concentrations in the eastern part of Texas, USA, Air Quality Atmosphere and Health, 8, 81-96,https://doi.org/10.1007/s11869-014-0276-5, 2015.

Grell, G. A.: PROGNOSTIC EVALUATION OF ASSUMPTIONS USED BY CUMULUS PARAMETERIZATIONS, Monthly Weather Review, 121, 764-787,https://doi.org/10.1175/1520-0493(1993)121<0764:Peoaub>2.0.Co;2, 1993.

Guan, Y. R., Shan, Y. L., Huang, Q., Chen, H. L., Wang, D., and Hubacek, K.: Assessment to

China's Recent Emission Pattern Shifts, Earths Future, 9,https://doi.org/10.1029/2021ef002241, 2021.

Guenther, A. B., Monson, R. K., and Fall, R.: ISOPRENE AND MONOTERPENE EMISSION RATE VARIABILITY - OBSERVATIONS WITH EUCALYPTUS AND EMISSION RATE ALGORITHM DEVELOPMENT, Journal of Geophysical Research-Atmospheres, 96, 10799-10808,https://doi.org/10.1029/91jd00960, 1991.

Guo, J. P., Miao, Y. C., Zhang, Y., Liu, H., Li, Z. Q., Zhang, W. C., He, J., Lou, M. Y., Yan, Y., Bian, L. G., and Zhai, P.: The climatology of planetary boundary layer height in China derived from radiosonde and reanalysis data, Atmospheric Chemistry and Physics, 16, 13309-13319,https://doi.org/10.5194/acp-16-13309-2016, 2016.

Haman, C. L., Couzo, E., Flynn, J. H., Vizuete, W., Heffron, B., and Lefer, B. L.: Relationship between boundary layer heights and growth rates with ground-level ozone in Houston, Texas, Journal of Geophysical Research-Atmospheres, 119, 6230-6245,https://doi.org/10.1002/2013jd020473, 2014.

Han, H., Liu, J., Shu, L., Wang, T., and Yuan, H.: Local and synoptic meteorological influences on daily variability in summertime surface ozone in eastern China, Atmospheric Chemistry and Physics, 20, 203-222,https://doi.org/10.5194/acp-20-203-2020, 2020.

He, J. W., Wang, Y. X., Hao, J. M., Shen, L. L., and Wang, L.: Variations of surface O-3 in August at a rural site near Shanghai: influences from the West Pacific subtropical high and anthropogenic emissions, Environmental Science and Pollution Research, 19, 4016-4029,https://doi.org/10.1007/s11356-012-0970-5, 2012.

Heald, C. L., Wilkinson, M. J., Monson, R. K., Alo, C. A., Wang, G. L., and Guenther, A.: Response of isoprene emission to ambient CO2 changes and implications for global budgets, Global Change Biology, 15, 1127-1140,https://doi.org/10.1111/j.1365-2486.2008.01802.x, 2009.

Hoffmann, L., Gunther, G., Li, D., Stein, O., Wu, X., Griessbach, S., Heng, Y., Konopka, P., Muller, R., Vogel, B., and Wright, J. S.: From ERA-Interim to ERA5: the considerable impact of ECMWF's next-generation reanalysis on Lagrangian transport simulations, Atmospheric Chemistry and Physics, 19, 3097-3124,https://doi.org/10.5194/acp-19-3097-2019, 2019.

Hong, C. P., Zhang, Q., He, K. B., Guan, D. B., Li, M., Liu, F., and Zheng, B.: Variations of China's emission estimates: response to uncertainties in energy statistics, Atmospheric Chemistry and Physics, 17, 1227-1239,https://doi.org/10.5194/acp-17-1227-2017, 2017.

IPCC (Ed.) Intergovernmental Panel on Climate Change (IPCC) (2021), the Physical Science Basis. Contribution of Working Group I to the Sixth Assessment Report of the Intergovernmental Panel on Climate Change, Cambridge University Press,Cambridge, United Kingdom and New York, NY, USA. , 2021.

Jacob, D. J. and Winner, D. A.: Effect of climate change on air quality, Atmospheric Environment, 43, 51-63,https://doi.org/10.1016/j.atmosenv.2008.09.051, 2009.

Jacobs, N., Simpson, W. R., Graham, K. A., Holmes, C., Hase, F., Blumenstock, T., Tu, Q., Frey, M., Dubey, M. K., Parker, H. A., Wunch, D., Kivi, R., Heikkinen, P., Notholt, J., Petri, C., and Warneke, T.: Spatial distributions of X-CO2 seasonal cycle amplitude and phase over northern high-latitude regions, Atmospheric Chemistry and Physics, 21, 16661-16687,https://doi.org/10.5194/acp-21-16661-2021, 2021.

Jiang, X., Wiedinmyer, C., and Carlton, A. G.: Aerosols from Fires: An Examination of the Effects on Ozone Photochemistry in the Western United States, Environmental Science &

688   Technology, 46, 11878-11886,https://doi.org/10.1021/es301541k, 2012.

689 KhayatianYazdi, F., Kamali, G., Mirrokni, S. M., and Memarian, M. H.: Sensitivity evaluation of
690   the different physical parameterizations schemes in regional climate model RegCM4.5
691   for simulation of air temperature and precipitation over North and West of Iran,
692   Dynamics of Atmospheres and Oceans,
693   93,https://doi.org/10.1016/j.dynatmoce.2020.101199, 2021.

694 Kong, L., Tang, X., Zhu, J., Wang, Z., Li, J., Wu, H., Wu, Q., Chen, H., Zhu, L., Wang, W., Liu,
695   B., Wang, Q., Chen, D., Pan, Y., Song, T., Li, F., Zheng, H., Jia, G., Lu, M., Wu, L., and
696   Carmichael, G. R.: A 6-year-long (2013-2018) high-resolution air quality reanalysis
697   dataset in China based on the assimilation of surface observations from CNEMC, Earth
698   System Science Data, 13, 529-570,https://doi.org/10.5194/essd-13-529-2021, 2021.

699 Lee, Y. C., Shindell, D. T., Faluvegi, G., Wenig, M., Lam, Y. F., Ning, Z., Hao, S., and Lai, C. S.:
700   Increase of ozone concentrations, its temperature sensitivity and the precursor factor in
701   South China, Tellus Series B-Chemical and Physical Meteorology,
702   66,https://doi.org/10.3402/tellusb.v66.23455, 2014.

703 Lefer, B. L., Shetter, R. E., Hall, S. R., Crawford, J. H., and Olson, J. R.: Impact of clouds and
704   aerosols on photolysis frequencies and photochemistry during TRACE-P: 1. Analysis
705   using radiative transfer and photochemical box models, Journal of Geophysical Research-
706   Atmospheres, 108,https://doi.org/10.1029/2002jd003171, 2003.

707 Lelieveld, J. and Crutzen, P. J.: INFLUENCES OF CLOUD PHOTOCHEMICAL PROCESSES
708   ON TROPOSPHERIC OZONE, Nature, 343, 227-233,https://doi.org/10.1038/343227a0,
709   1990.

710 Li, J., Chen, X. S., Wang, Z. F., Du, H. Y., Yang, W. Y., Sun, Y. L., Hu, B., Li, J. J., Wang, W.,
711   Wang, T., Fu, P. Q., and Huang, H. L.: Radiative and heterogeneous chemical effects of
712   aerosols on ozone and inorganic aerosols over East Asia, Science of the Total
713   Environment, 622, 1327-1342,https://doi.org/10.1016/j.scitotenv.2017.12.041, 2018.

714 Li, K., Jacob, D. J., Liao, H., Shen, L., Zhang, Q., and Bates, K. H.: Anthropogenic drivers of
715   2013-2017 trends in summer surface ozone in China, Proceedings of the National
716   Academy of Sciences of the United States of America, 116, 422-
717   427,https://doi.org/10.1073/pnas.1812168116, 2019.

718 Li, K., Jacob, D. J., Shen, L., Lu, X., De Smedt, I., and Liao, H.: Increases in surface ozone
719   pollution in China from 2013 to 2019: anthropogenic and meteorological influences,
720   Atmospheric Chemistry and Physics, 20, 11423-11433,https://doi.org/10.5194/acp-20-
721   11423-2020, 2020.

722 Li, R., Zhang, M., Chen, L., Kou, X., and Skorokhod, A.: CMAQ simulation of atmospheric
723   CO2 concentration in East Asia: Comparison with GOSAT observations and ground
724   measurements, Atmospheric Environment, 160, 176-
725   185,https://doi.org/10.1016/j.atmosenv.2017.03.056, 2017.

726 Li, X. B., Yuan, B., Parrish, D. D., Chen, D. H., Song, Y. X., Yang, S. X., Liu, Z. J., and Shao, M.:
727   Long-term trend of ozone in southern China reveals future mitigation strategy for air
728   pollution, Atmospheric Environment,
729   269,https://doi.org/10.1016/j.atmosenv.2021.118869, 2022.

730 Lin, J.-T., Patten, K. O., Hayhoe, K., Liang, X.-Z., and Wuebbles, D. J.: Effects of future climate
731   and biogenic emissions changes on surface ozone over the United States and China,
732   Journal of Applied Meteorology and Climatology, 47, 1888-
733   1909,https://doi.org/10.1175/2007jamc1681.1, 2008.

Liu, C. H., Ikeda, K., Rasmussen, R., Barlage, M., Newman, A. J., Prein, A. F., Chen, F., Chen, L., Clark, M., Dai, A. G., Dudhia, J., Eidhammer, T., Gochis, D., Gutmann, E., Kurkute, S., Li, Y. P., Thompson, G., and Yates, D.: Continental-scale convection-permitting modeling of the current and future climate of North America, Climate Dynamics, 49, 71-95,https://doi.org/10.1007/s00382-016-3327-9, 2017.

Liu, H., Liu, S., Xue, B., Lv, Z., Meng, Z., Yang, X., Xue, T., Yu, Q., and He, K.: Ground-level ozone pollution and its health impacts in China, Atmospheric Environment, 173, 223-230,https://doi.org/10.1016/j.atmosenv.2017.11.014, 2018a.

Liu, L., Zhou, L., Zhang, X., Wen, M., Zhang, F., Yao, B., and Fang, S.: The characteristics of atmospheric CO_2 concentration variation of four national background stations in China, Science in China Series D-Earth Sciences, 52, 1857-1863,https://doi.org/10.1007/s11430-009-0143-7, 2009.

Liu, Y. and Wang, T.: Worsening urban ozone pollution in China from 2013 to 2017-Part 1: The complex and varying roles of meteorology, Atmospheric Chemistry and Physics, 20, 6305-6321,https://doi.org/10.5194/acp-20-6305-2020, 2020a.

Liu, Y. and Wang, T.: Worsening urban ozone pollution in China from 2013 to 2017-Part 2: The effects of emission changes and implications for multi-pollutant control, Atmospheric Chemistry and Physics, 20, 6323-6337,https://doi.org/10.5194/acp-20-6323-2020, 2020b.

Liu, Z., Liu, Y., Wang, S., Yang, X., Wang, L., Baig, M. H. A., Chi, W., and Wang, Z.: Evaluation of Spatial and Temporal Performances of ERA-Interim Precipitation and Temperature in Mainland China, Journal of Climate, 31, 4347-4365,https://doi.org/10.1175/jcli-d-17-0212.1, 2018b.

Lu, H., Yi, S., Liu, Z., Mason, J. A., Jiang, D., Cheng, J., Stevens, T., Xu, Z., Zhang, E., Jin, L., Zhang, Z., Guo, Z., Wang, Y., and Otto-Bliesner, B.: Variation of East Asian monsoon precipitation during the past 21 k.y. and potential CO_2 forcing, Geology, 41, 1023-1026,https://doi.org/10.1130/g34488.1, 2013.

Lu, X., Zhang, L., Wang, X. L., Gao, M., Li, K., Zhang, Y. Z., Yue, X., and Zhang, Y. H.: Rapid Increases in Warm-Season Surface Ozone and Resulting Health Impact in China Since 2013, Environmental Science & Technology Letters, 7, 240-247,https://doi.org/10.1021/acs.estlett.0c00171, 2020.

Lu, X., Hong, J., Zhang, L., Cooper, O. R., Schultz, M. G., Xu, X., Wang, T., Gao, M., Zhao, Y., and Zhang, Y.: Severe Surface Ozone Pollution in China: A Global Perspective, Environmental Science & Technology Letters, 5, 487-494,https://doi.org/10.1021/acs.estlett.8b00366, 2018.

Lu, X., Zhang, L., Chen, Y. F., Zhou, M., Zheng, B., Li, K., Liu, Y. M., Lin, J. T., Fu, T. M., and Zhang, Q.: Exploring 2016-2017 surface ozone pollution over China: source contributions and meteorological influences, Atmospheric Chemistry and Physics, 19, 8339-8361,https://doi.org/10.5194/acp-19-8339-2019, 2019.

Lv, Q., Liu, H. B., Wang, J. T., Liu, H., and Shang, Y.: Multiscale analysis on spatiotemporal dynamics of energy consumption CO_2 emissions in China: Utilizing the integrated of DMSP-OLS and NPP-VIIRS nighttime light datasets, Science of the Total Environment, 703,https://doi.org/10.1016/j.scitotenv.2019.134394, 2020.

Ma, D., Wang, T., Xu, B., Song, R., Gao, L., Chen, H., Ren, X., Li, S., Zhuang, B., and Li, M.: The mutual interactions among ozone, fine particulate matter, and carbon dioxide on summer monsoon climate in East Asia, Atmospheric Environment, 119668, 2023.

Ma, Z., Xu, J., Quan, W., Zhang, Z., Lin, W., and Xu, X.: Significant increase of surface ozone at

780 a rural site, north of eastern China, Atmospheric Chemistry and Physics, 16, 3969-
781   3977,https://doi.org/10.5194/acp-16-3969-2016, 2016.
782 Monks, P. S., Archibald, A. T., Colette, A., Cooper, O., Coyle, M., Derwent, R., Fowler, D.,
783   Granier, C., Law, K. S., Mills, G. E., Stevenson, D. S., Tarasova, O., Thouret, V., von
784   Schneidemesser, E., Sommariva, R., Wild, O., and Williams, M. L.: Tropospheric ozone
785   and its precursors from the urban to the global scale from air quality to short-lived
786   climate forcer, Atmos. Chem. Phys., 15, 8889-8973,https://doi.org/10.5194/acp-15-8889-
787   2015, 2015.
788 Monson, R. K. and Fall, R.: ISOPRENE EMISSION FROM ASPEN LEAVES - INFLUENCE
789   OF ENVIRONMENT AND RELATION TO PHOTOSYNTHESIS AND
790   PHOTORESPIRATION, Plant Physiology, 90, 267-
791   274,https://doi.org/10.1104/pp.90.1.267, 1989.
792 Mousavinezhad, S., Choi, Y., Pouyaei, A., Ghahremanloo, M., and Nelson, D. L.: A
793   comprehensive investigation of surface ozone pollution in China, 2015-2019: Separating
794   the contributions from meteorology and precursor emissions, Atmospheric Research,
795   257,https://doi.org/10.1016/j.atmosres.2021.105599, 2021.
796 Pfister, G. G., Walters, S., Lamarque, J. F., Fast, J., Barth, M. C., Wong, J., Done, J., Holland, G.,
797   and Bruyere, C. L.: Projections of future summertime ozone over the US, Journal of
798   Geophysical Research-Atmospheres, 119, 5559-
799   5582,https://doi.org/10.1002/2013jd020932, 2014.
800 Possell, M., Hewitt, C. N., and Beerling, D. J.: The effects of glacial atmospheric CO2
801   concentrations and climate on isoprene emissions by vascular plants, Global Change
802   Biology, 11, 60-69,https://doi.org/10.1111/j.1365-2486.2004.00889.x, 2005.
803 Pu, X., Wang, T. J., Huang, X., Melas, D., Zanis, P., Papanastasiou, D. K., and Poupkou, A.:
804   Enhanced surface ozone during the heat wave of 2013 in Yangtze River Delta region,
805   China, Science of the Total Environment, 603, 807-
806   816,https://doi.org/10.1016/j.scitotenv.2017.03.056, 2017.
807 Rapparini, F., Baraldi, R., Miglietta, F., and Loreto, F.: Isoprenoid emission in trees of Quercus
808   pubescens and Quercus ilex with lifetime exposure to naturally high CO2 environment,
809   Plant Cell and Environment, 27, 381-391,https://doi.org/10.1111/j.1365-
810   3040.2003.01151.x, 2004.
811 Ren, S. G., Yuan, B. L., Ma, X., and Chen, X. H.: International trade, FDI (foreign direct
812   investment) and embodied CO2 emissions: A case study of Chinas industrial sectors,
813   China Economic Review, 28, 123-134,https://doi.org/10.1016/j.chieco.2014.01.003, 2014.
814 Reynolds, R. W., Rayner, N. A., Smith, T. M., Stokes, D. C., and Wang, W. Q.: An improved in
815   situ and satellite SST analysis for climate, Journal of Climate, 15, 1609-
816   1625,https://doi.org/10.1175/1520-0442(2002)015<1609:Aiisas>2.0.Co;2, 2002.
817 Rosenstiel, T. N., Potosnak, M. J., Griffin, K. L., Fall, R., and Monson, R. K.: Increased CO2
818   uncouples growth from isoprene emission in an agriforest ecosystem, Nature, 421, 256-
819   259,https://doi.org/10.1038/nature01312, 2003.
820 Sanchez-Ccoyllo, O. R., Ynoue, R. Y., Martins, L. D., and Andrade, M. d. F.: Impacts of ozone
821   precursor limitation and meteorological variables on ozone concentration in Sao Paulo,
822   Brazil, Atmospheric Environment, 40, S552-
823   S562,https://doi.org/10.1016/j.atmosenv.2006.04.069, 2006.
824 Schimel, D., Stephens, B. B., and Fisher, J. B.: Effect of increasing CO2 on the terrestrial carbon
825   cycle, Proceedings of the National Academy of Sciences of the United States of America,

112, 436-441,https://doi.org/10.1073/pnas.1407302112, 2015.

Shalaby, A., Zakey, A. S., Tawfik, A. B., Solmon, F., Giorgi, F., Stordal, F., Sillman, S., Zaveri, R. A., and Steiner, A. L.: Implementation and evaluation of online gas-phase chemistry within a regional climate model (RegCM-CHEM4), Geoscientific Model Development, 5, 741-760,https://doi.org/10.5194/gmd-5-741-2012, 2012.

Sharkey, T. D., Loreto, F., and Delwiche, C. F.: HIGH-CARBON DIOXIDE AND SUN SHADE EFFECTS ON ISOPRENE EMISSION FROM OAK AND ASPEN TREE LEAVES, Plant Cell and Environment, 14, 333-338,https://doi.org/10.1111/j.1365-3040.1991.tb01509.x, 1991.

Shen, L., Mickley, L. J., and Gilleland, E.: Impact of increasing heat waves on US ozone episodes in the 2050s: Results from a multimodel analysis using extreme value theory, Geophysical Research Letters, 43, 4017-4025,https://doi.org/10.1002/2016gl068432, 2016.

Shen, L., Jacob, D. J., Liu, X., Huang, G., Li, K., Liao, H., and Wang, T.: An evaluation of the ability of the Ozone Monitoring Instrument (OMI) to observe boundary layer ozone pollution across China: application to 2005-2017 ozone trends, Atmospheric Chemistry and Physics, 19, 6551-6560,https://doi.org/10.5194/acp-19-6551-2019, 2019.

Shen, L., Liu, J., Zhao, T., Xu, X., Han, H., Wang, H., and Shu, Z.: Atmospheric transport drives regional interactions of ozone pollution in China, Science of the Total Environment, 830,https://doi.org/10.1016/j.scitotenv.2022.154634, 2022.

Shetter, R. E., Cinquini, L., Lefer, B. L., Hall, S. R., and Madronich, S.: Comparison of airborne measured and calculated spectral actinic flux and derived photolysis frequencies during the PEM Tropics B mission, Journal of Geophysical Research-Atmospheres, 108,https://doi.org/10.1029/2001jd001320, 2002.

Shi, K. F., Chen, Y., Yu, B. L., Xu, T. B., Chen, Z. Q., Liu, R., Li, L. Y., and Wu, J. P.: Modeling spatiotemporal CO2 (carbon dioxide) emission dynamics in China from DMSP-OLS nighttime stable light data using panel data analysis, Applied Energy, 168, 523-533,https://doi.org/10.1016/j.apenergy.2015.11.055, 2016.

Singh, S. and Singh, R.: High-altitude clear-sky direct solar ultraviolet irradiance at Leh and Hanle in the western Himalayas: Observations and model calculations, Journal of Geophysical Research-Atmospheres, 109,https://doi.org/10.1029/2004jd004854, 2004.

Steiner, A. L., Davis, A. J., Sillman, S., Owen, R. C., Michalak, A. M., and Fiore, A. M.: Observed suppression of ozone formation at extremely high temperatures due to chemical and biophysical feedbacks, Proceedings of the National Academy of Sciences of the United States of America, 107, 19685-19690,https://doi.org/10.1073/pnas.1008336107, 2010.

Sun, Z. H., Hve, K., Vislap, V., and Niinemets, U.: Elevated CO2 magnifies isoprene emissions under heat and improves thermal resistance in hybrid aspen, Journal of Experimental Botany, 64, 5509-5523,https://doi.org/10.1093/jxb/ert318, 2013.

Tai, A. P. K., Mickley, L. J., Heald, C. L., and Wu, S. L.: Effect of CO2 inhibition on biogenic isoprene emission: Implications for air quality under 2000 to 2050 changes in climate, vegetation, and land use, Geophysical Research Letters, 40, 3479-3483,https://doi.org/10.1002/grl.50650, 2013.

Tie, X. X., Madronich, S., Walters, S., Zhang, R. Y., Rasch, P., and Collins, W.: Effect of clouds on photolysis and oxidants in the troposphere, Journal of Geophysical Research-Atmospheres, 108,https://doi.org/10.1029/2003jd003659, 2003.

872   Verstraeten, W. W., Neu, J. L., Williams, J. E., Bowman, K. W., Worden, J. R., and Boersma, K.
873   F.: Rapid increases in tropospheric ozone production and export from China (vol 8, pg
874   690, 2015), Nature Geoscience, 9, 643-643,https://doi.org/10.1038/ngeo2768, 2016.
875   Wang, L. T., Wei, Z., Yang, J., Zhang, Y., Zhang, F. F., Su, J., Meng, C. C., and Zhang, Q.: The
876   2013 severe haze over southern Hebei, China: model evaluation, source apportionment,
877   and policy implications, Atmospheric Chemistry and Physics, 14, 3151-
878   3173,https://doi.org/10.5194/acp-14-3151-2014, 2014.
879   Wang, N., Lyu, X. P., Deng, X. J., Huang, X., Jiang, F., and Ding, A. J.: Aggravating O-3
880   pollution due to NOx emission control in eastern China, Science of the Total
881   Environment, 677, 732-744,https://doi.org/10.1016/j.scitotenv.2019.04.388, 2019a.
882   Wang, P., Guo, H., Hu, J., Kota, S. H., Ying, Q., and Zhang, H.: Responses of PM2.5 and O-3
883   concentrations to changes of meteorology and emissions in China, Science of the Total
884   Environment, 662, 297-306,https://doi.org/10.1016/j.scitotenv.2019.01.227, 2019b.
885   Wang, T., Dai, J., Lam, K. S., Nan Poon, C., and Brasseur, G. P.: Twenty-Five Years of Lower
886   Tropospheric Ozone Observations in Tropical East Asia: The Influence of Emissions and
887   Weather Patterns, Geophysical Research Letters, 46, 11463-
888   11470,https://doi.org/10.1029/2019gl084459, 2019c.
889   Wang, T., Xue, L., Brimblecombe, P., Lam, Y. F., Li, L., and Zhang, L.: Ozone pollution in China:
890   A review of concentrations, meteorological influences, chemical precursors, and effects,
891   Science of the Total Environment, 575, 1582-
892   1596,https://doi.org/10.1016/j.scitotenv.2016.10.081, 2017a.
893   Wang, W. N., Cheng, T. H., Gu, X. F., Chen, H., Guo, H., Wang, Y., Bao, F. W., Shi, S. Y., Xu, B.
894   R., Zuo, X., Meng, C., and Zhang, X. C.: Assessing Spatial and Temporal Patterns of
895   Observed Ground-level Ozone in China, Scientific Reports,
896   7,https://doi.org/10.1038/s41598-017-03929-w, 2017b.
897   Wang, X., Chen, F., Wu, Z., Zhang, M., Tewari, M., Guenther, A., and Wiedinmyer, C.: Impacts
898   of Weather Conditions Modified by Urban Expansion on Surface Ozone: Comparison
899   between the Pearl River Delta and Yangtze River Delta Regions, Advances in
900   Atmospheric Sciences, 26, 962-972,https://doi.org/10.1007/s00376-009-8001-2, 2009.
901   Wang, Y., Chen, H., Wu, Q., Chen, X., Wang, H., Gbaguidi, A., Wang, W., and Wang, Z.: Three-
902   year, 5 km resolution China PM2.5 simulation: Model performance evaluation,
903   Atmospheric Research, 207, 1-13,https://doi.org/10.1016/j.atmosres.2018.02.016, 2018.
904   Wang, Y., Gao, W., Wang, S., Song, T., Gong, Z., Ji, D., Wang, L., Liu, Z., Tang, G., Huo, Y.,
905   Tian, S., Li, J., Li, M., Yang, Y., Chu, B., Petaja, T., Kerminen, V.-M., He, H., Hao, J.,
906   Kulmala, M., Wang, Y., and Zhang, Y.: Contrasting trends of PM2.5 and surface-ozone
907   concentrations in China from 2013 to 2017, National Science Review, 7, 1331-
908   1339,https://doi.org/10.1093/nsr/nwaa032, 2020.
909   Wei, J., Li, Z. Q., Li, K., Dickerson, R. R., Pinker, R. T., Wang, J., Liu, X., Sun, L., Xue, W. H.,
910   and Cribb, M.: Full-coverage mapping and spatiotemporal variations of ground-level
911   ozone (O3) pollution from 2013 to 2020 across China, Remote Sensing of Environment,
912   270,https://doi.org/10.1016/j.rse.2021.112775, 2022.
913   Wilkinson, M. J., Monson, R. K., Trahan, N., Lee, S., Brown, E., Jackson, R. B., Polley, H. W.,
914   Fay, P. A., and Fall, R.: Leaf isoprene emission rate as a function of atmospheric CO2
915   concentration, Global Change Biology, 15, 1189-1200,https://doi.org/10.1111/j.1365-
916   2486.2008.01803.x, 2009.
917   Wu, W., Xue, W., Lei, Y., and Wang, J.: Sensitivity analysis of ozone in Beijing-Tianjin-Hebei

918   (BTH) and its surrounding area using OMI satellite remote sensing data, China
919   Environmental Science, 38, 1201-1208, 2018.
920 Xie, X., Huang, X., Wang, T., Li, M., Li, S., and Chen, P.: Simulation of Non-Homogeneous
921   CO2 and Its Impact on Regional Temperature in East Asia, Journal of Meteorological
922   Research, 32, 456-468,https://doi.org/10.1007/s13351-018-7159-x, 2018.
923 Xie, X., Wang, T., Yue, X., Li, S., Zhuang, B., and Wang, M.: Effects of atmospheric aerosols on
924   terrestrial carbon fluxes and CO2 concentrations in China, Atmospheric Research,
925   237,https://doi.org/10.1016/j.atmosres.2020.104859, 2020.
926 Xie, X., Wang, T., Yue, X., Li, S., Zhuang, B., Wang, M., and Yang, X.: Numerical modeling of
927   ozone damage to plants and its effects on atmospheric CO2 in China, Atmospheric
928   Environment, 217,https://doi.org/10.1016/j.atmosenv.2019.116970, 2019.
929 Xu, B., Wang, T., Ma, D., Song, R., Zhang, M., Gao, L., Li, S., Zhuang, B., Li, M., and Xie, M.:
930   Impacts of regional emission reduction and global climate change on air quality and
931   temperature to attain carbon neutrality in China, Atmospheric Research,
932   279,https://doi.org/10.1016/j.atmosres.2022.106384, 2022a.
933 Xu, B. Y., Wang, T. J., Ma, D. Y., Song, R., Zhang, M., Gao, L. B., Li, S., Zhuang, B. L., Li, M.
934   M., and Xie, M.: Impacts of regional emission reduction and global climate change on air
935   quality and temperature to attain carbon neutrality in China, Atmospheric Research,
936   279,https://doi.org/10.1016/j.atmosres.2022.106384, 2022b.
937 Xu, W., Xu, X., Lin, M., Lin, W., Tarasick, D., Tang, J., Ma, J., and Zheng, X.: Long-term trends
938   of surface ozone and its influencing factors at the Mt Waliguan GAW station, China - Part
939   2: The roles of anthropogenic emissions and climate variability, Atmospheric Chemistry
940   and Physics, 18, 773-798,https://doi.org/10.5194/acp-18-773-2018, 2018.
941 Yang, Y., Liao, H., and Li, J.: Impacts of the East Asian summer monsoon on interannual
942   variations of summertime surface-layer ozone concentrations over China, Atmospheric
943   Chemistry and Physics, 14, 6867-6879,https://doi.org/10.5194/acp-14-6867-2014, 2014.
944 Yin, C., Wang, T., Solmon, F., Mallet, M., and Zhuang, B.: Assessment of direct radiative forcing
945   due to secondary organic aerosol over China with a regional climate model, Tellus Series
946   B-chemical & Physical Meteorology, 67,https://doi.org/10.3402/tellusb.v67.24634, 2015.
947 Yin, Z. and Ma, X.: Meteorological conditions contributed to changes in dominant patterns of
948   summer ozone pollution in Eastern China, Environmental Research Letters,
949   15,https://doi.org/10.1088/1748-9326/abc915, 2020.
950 Yoo, J. M., Lee, Y. R., Kim, D., Jeong, M. J., Stockwell, W. R., Kundu, P. K., Oh, S. M., Shin, D.
951   B., and Lee, S. J.: New indices for wet scavenging of air pollutants (O-3, CO, NO2, SO2,
952   and PM10) by summertime rain, Atmospheric Environment, 82, 226-
953   237,https://doi.org/10.1016/j.atmosenv.2013.10.022, 2014.
954 Yue, X. and Unger, N.: The Yale Interactive terrestrial Biosphere model version 1.0: description,
955   evaluation and implementation into NASA GISS ModelE2, Geoscientific Model
956   Development,https://doi.org/10.5194/gmd-8-2399-2015, 2015.
957 Zaveri, R. A. and Peters, L. K.: A new lumped structure photochemical mechanism for large-
958   scale applications, Journal of Geophysical Research Atmospheres, 104, 30387-
959   30415,https://doi.org/10.1029/1999JD900876, 1999.
960 Zhai, S. X., Jacob, D. J., Wang, X., Shen, L., Li, K., Zhang, Y. Z., Gui, K., Zhao, T. L., and Liao,
961   H.: Fine particulate matter (PM2.5) trends in China, 2013-2018: separating contributions
962   from anthropogenic emissions and meteorology, Atmospheric Chemistry and Physics, 19,
963   11031-11041,https://doi.org/10.5194/acp-19-11031-2019, 2019.

964   Zhao, S., Yu, Y., Yin, D., Qin, D., He, J., and Dong, L.: Spatial patterns and temporal variations
965   of six criteria air pollutants during 2015 to 2017 in the city clusters of Sichuan Basin,
966   China, Science of the Total Environment, 624, 540-
967   557,https://doi.org/10.1016/j.scitotenv.2017.12.172, 2018.
968   Zheng, B., Tong, D., Li, M., Liu, F., Hong, C., Geng, G., Li, H., Li, X., Peng, L., Qi, J., Yan, L.,
969   Zhang, Y., Zhao, H., Zheng, Y., He, K., and Zhang, Q.: Trends in China's anthropogenic
970   emissions since 2010 as the consequence of clean air actions, Atmospheric Chemistry and
971   Physics, 18, 14095-14111,https://doi.org/10.5194/acp-18-14095-2018, 2018.
972   Zheng, J., Shao, M., Che, W., Zhang, L., Zhong, L., Zhang, Y., and Streets, D.: Speciated VOC
973   Emission Inventory and Spatial Patterns of Ozone Formation Potential in the Pearl River
974   Delta, China, Environmental Science & Technology, 43, 8580-
975   8586,https://doi.org/10.1021/es901688e, 2009.
976   Zheng, S., Cao, C. X., and Singh, R. P.: Comparison of ground based indices (API and AQI) with
977   satellite based aerosol products, Science of the Total Environment, 488, 400-
978   414,https://doi.org/10.1016/j.scitotenv.2013.12.074, 2014.
979   Zhuang, B. L., Li, S., Wang, T. J., Liu, J., Chen, H. M., Chen, P. L., Li, M. M., and Xie, M.:
980   Interaction between the Black Carbon Aerosol Warming Effect and East Asian Monsoon
981   Using RegCM4, Journal of Climate, 31, 9367-9388,https://doi.org/10.1175/jcli-d-17-
982   0767.1, 2018.
983